2020 Spring

Advanced Solidification

04.29.2020

Eun Soo Park

Office: 33-313
Telephone: 880-7221
Email: espark@snu.ac.kr
Office hours: by appointment

Contents for previous class

Equilibrium Shape and Interface Structure on an Atomic Scale

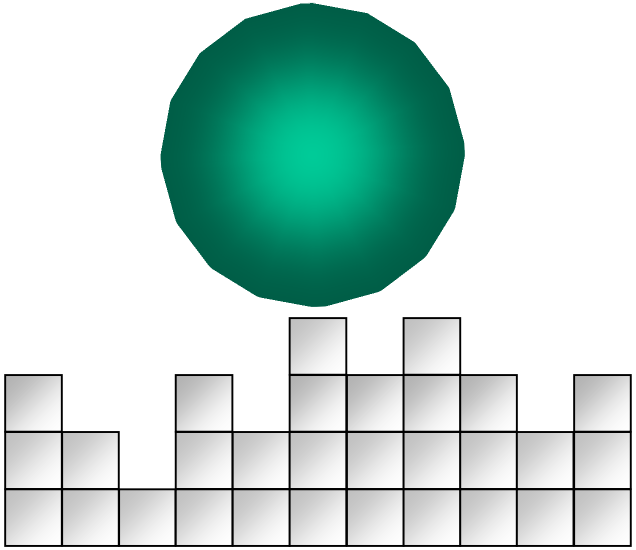

atomically-disordered

Ex) metallic systems

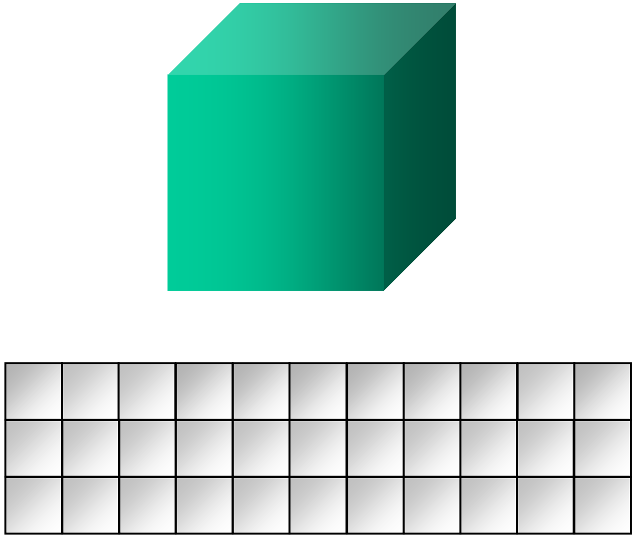

atomically-flat

nonmetals

Apply thermodynamics to this fact and derive more information.

Entropy-dominant

weak bonding energy

stable at high T

←

Enthalpy-dominant

strong bonding energy

stable at low T

Thermal Roughening

singular (smooth) interface

rough interface

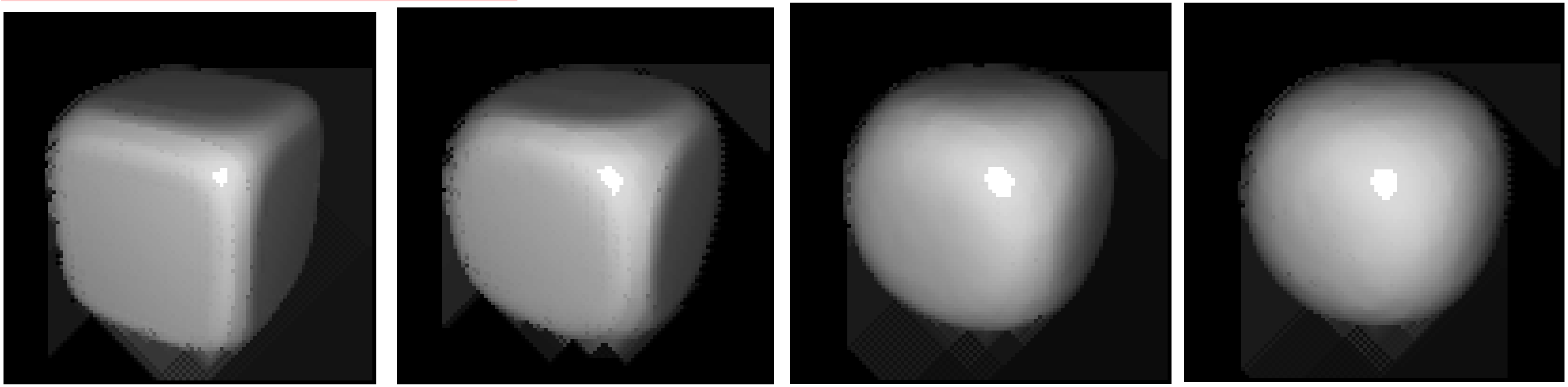

Enthalpy-dominant

Entropy-dominant

Heating up to the roughening transition.

Kinetic Roughening

Rough interface - Ideal Growth → diffusion-controlled → dendritic growth

Smooth interface - Growth by Screw Dislocation

Growth by 2-D Nucleation

Small ΔT → "feather" type of growth ⟷ Large ΔT → cellular/dendritic growth

The growth rate of the singular interface cannot be higher than ideal growth rate.

When the growth rate of the singular Interface is high enough, it follows the ideal growth rate like a rough interface.

→ kinetic roughening

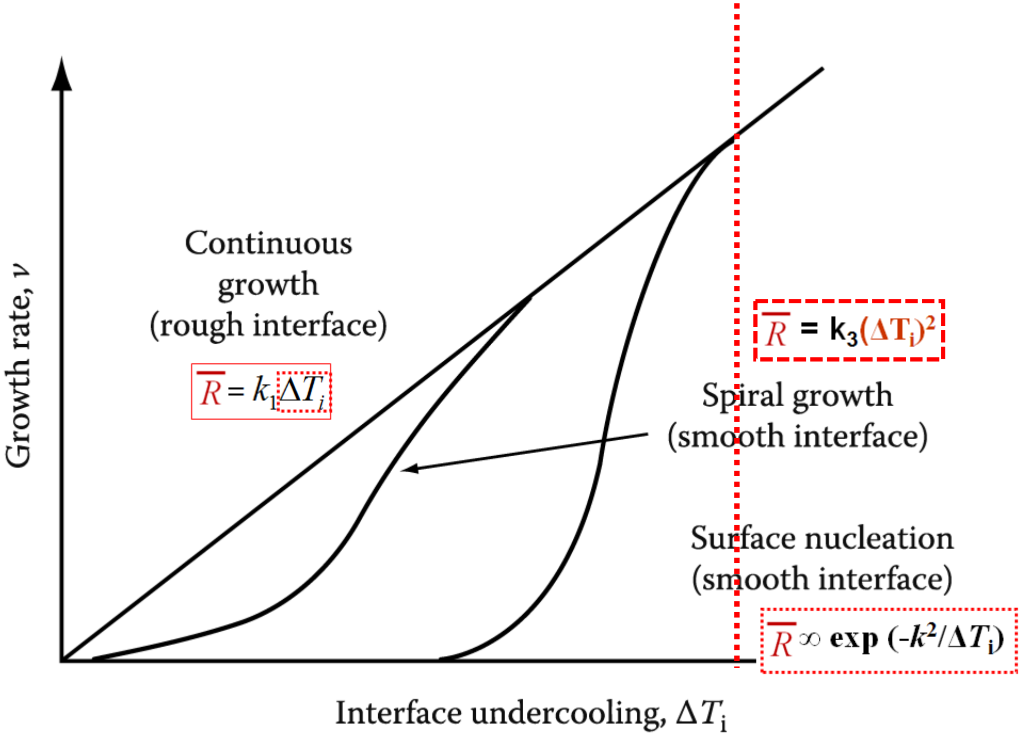

* Melting vs. Freezing at equilibrium temperature, T_E

*** Net rate, $\overline{R}$** = difference between R_M **and** R_F

$$= N_L A_F G_F \nu_L \exp(-Q_F/RT) - N_S A_M G_M \nu_S \exp(-Q_M/RT)$$

$$\boxed{\frac{L}{RT_E} = \ln\frac{A_M}{A_F}}$$

*** A_M ~ 1 for all liquid, A_F depends on crystal structure**

- **Metallic structure** (FCC, C.P.H, and BCC, "less localized bonding") ~ good relationship compared with the structures which are covalently bonded ("specific directional bonds").

- **Molecular liquid such as F_2, Cl_2 ~ extra condition for A_F**
  (∵ molecule must be correctly oriented in order to be accommodated.)

< Relationship btw latent heat and melting point>

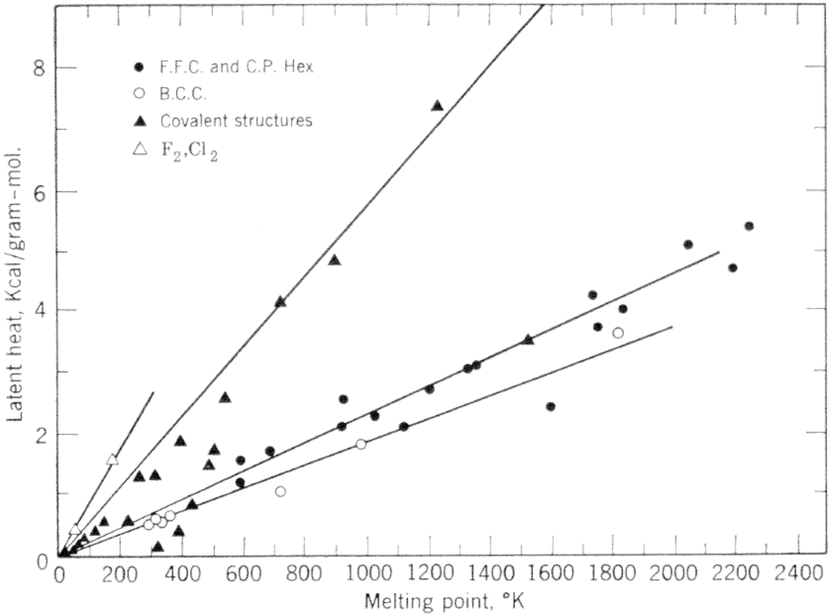

* Melting vs. Freezing at equilibrium temperature, T_E → Solid-Liquid Equilibrium in Alloys

From eqn. (102)

$$(S^s - S^l)\,\frac{\mathrm{d}T}{\mathrm{d}X_A} = 0.$$

Since $S^s \neq S^l$, then $\mathrm{d}T/\mathrm{d}X_A = 0$. Thus the condition $X_A^s = X_A^l$ is only associated with $\mathrm{d}T/\mathrm{d}X_A = 0$, *i.e.* with a minimum or a maximum in the line $T_A T_B$ of Fig. 22. Except for this particular case therefore $X_A^s \neq X_A^l$. There is a difference between the composition of the liquid and solid phase in the general case.

- **Consider the free energy curves for liquid and α phase at a temperature T, where $T_A > T > T_B$. The standard states are pure *solid* A and pure *liquid* B at temperature T. → Derive the free energy curves for the liquid and α phases.**

$$X_B^s - X_B^l = \frac{\Delta H_A}{R T_A^2}(T_A - T) \tag{106}$$

or,

$$\left(\frac{\mathrm{d}X_B^s}{\mathrm{d}T} - \frac{\mathrm{d}X_B^l}{\mathrm{d}T}\right)_{T=T_A} = \frac{\Delta H_A}{R T_A^2}. \tag{107}$$

Equations (106) and (107) are referred to as the Van't Hoff relation. They give the depression of the freezing point for a liquid solution in equilibrium with a solid solution. The difference in initial slopes of the solidus and liquidus curves, the slopes at $T = T_A$ and $X_A = 1$, are dependent on the latent heat of fusion of pure A (ΔH_A) but independent of the nature of the solute.

Assumption: complete mutual solid solubility

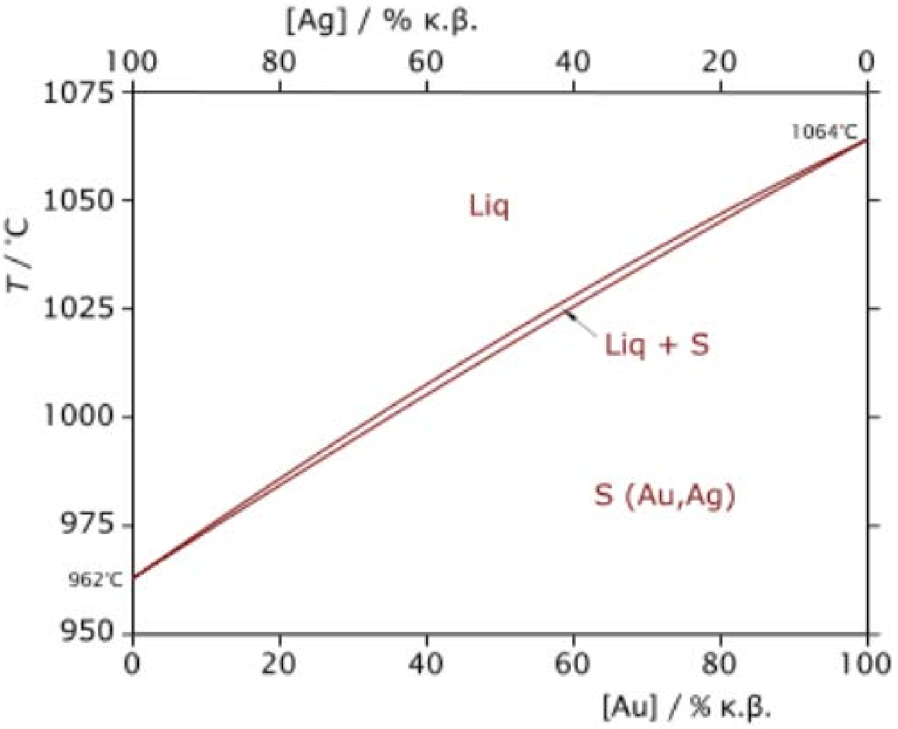

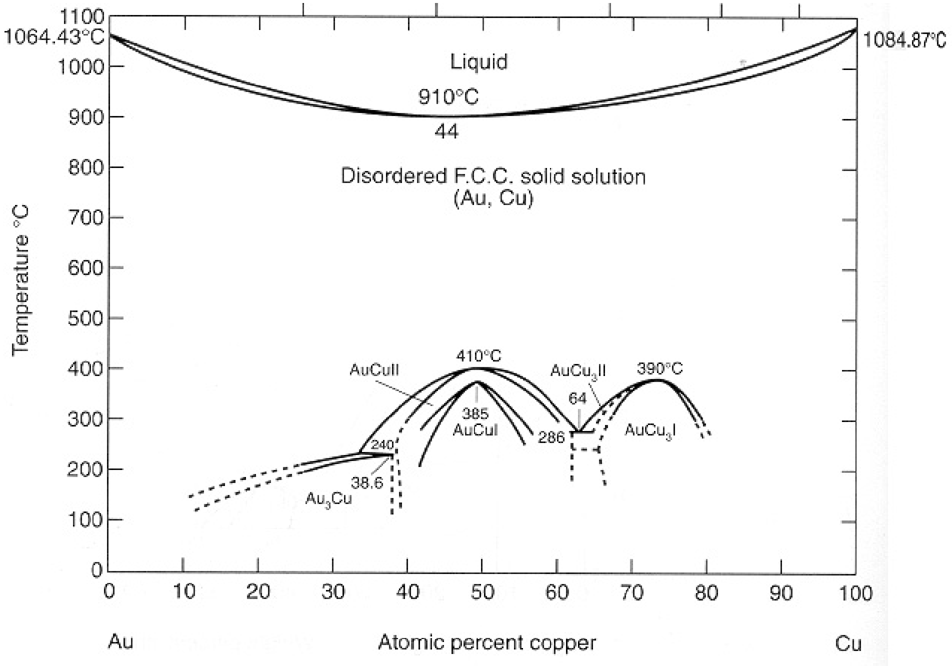

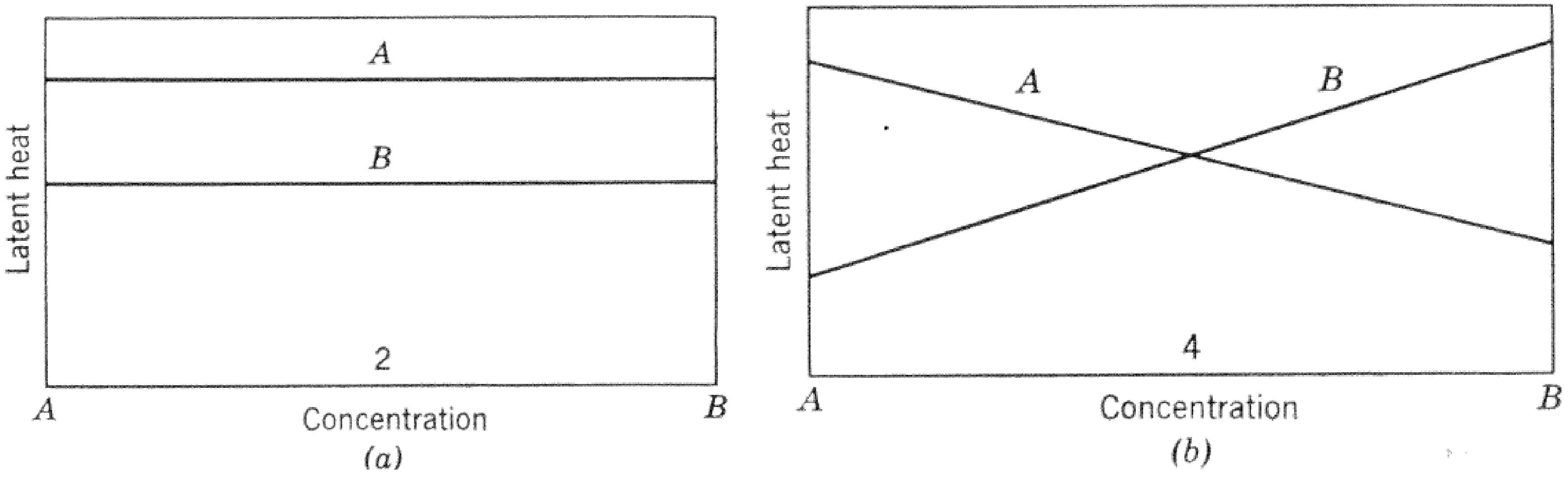

(a)

(b)

Fig. 2.14. Latent heat-concentration relationships for solid solutions. (From Ref. 24.)

Assumption: limited solid solubility, two different terminal crystal structures

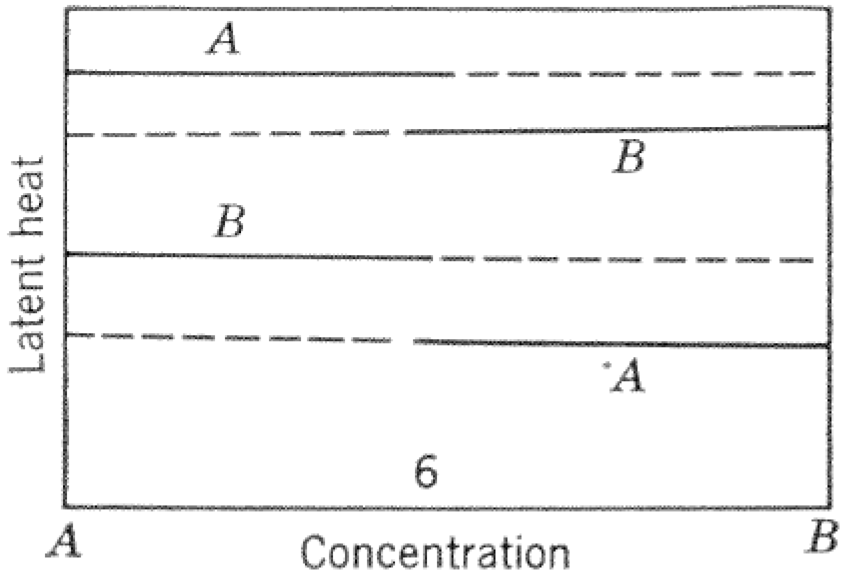

Fig. 2.16. Relationship between latent heat and concentration for an ideal eutectic forming system. (From Ref. 24.)

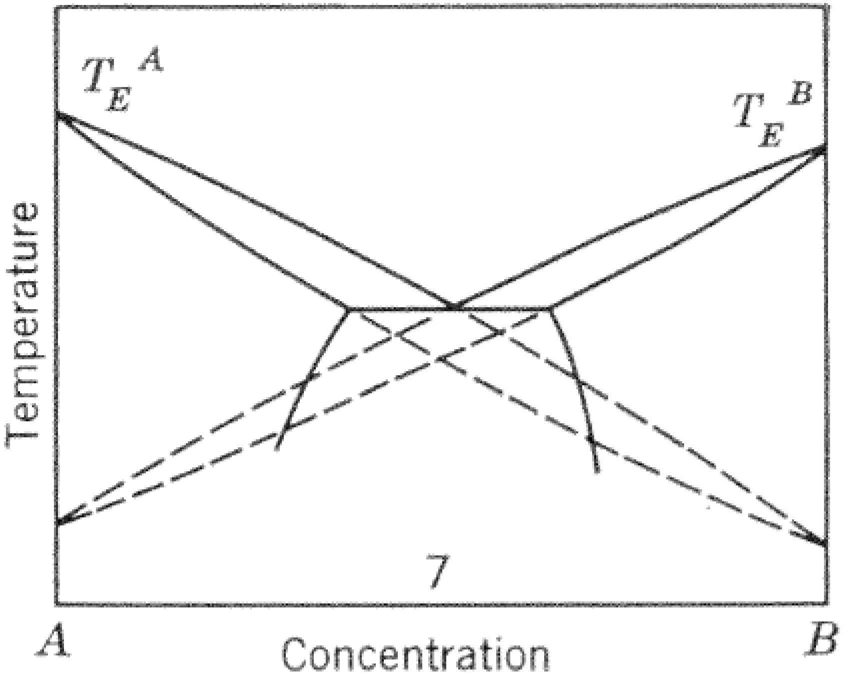

Fig. 2.17. Schematic phase diagram for eutectic forming system. (From Ref. 24.)

Contents for previous and today's class

* Two-Phase Equilibrium

→ Binary phase diagrams

* Origin of Defects

* Chapter 2 Solidification as an Atomistic Process

→ Chapter 3 Nucleation

- Metastability of Supercooled Liquids
- Equilibrium conditions for a curved interface
- Calculation of critical radius
- The process of Nucleation

- Two-Phase Equilibrium

1) Simple Phase Diagrams

Assumption: (1) completely miscible in solid and liquid.
(2) Both are ideal soln.
(3) $T_m(A) > T_m(B)$

$$\Delta H^{L}_{mix} = 0 \quad \Delta H^{S}_{mix} = 0$$

$$dG^s = V^s dP - S^s dT + \mu_A^s dX_A^s + \mu_B^s dX_B^s$$
$$dG^l = V^l dP - S^l dT + \mu_A^l dX_A^l + \mu_B^l dX_B^l.$$

At equilibrium

$$dG^s = dG^l, \quad \mu_A^s = \mu_A^l \quad \text{and} \quad \mu_B^s = \mu_B^l.$$

At constant P

$$-(S^s - S^l)\, dT = (\mu_A - \mu_B)(dX_A^l - dX_A^s).$$

Differentiating with respect to X_A,

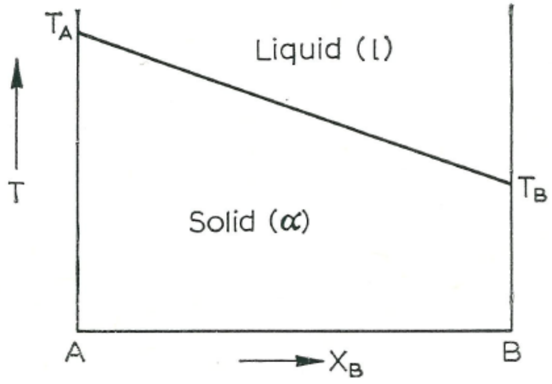

Fig. 22.

$$(S^s - S^l)\frac{dT}{dX_A} = (\mu_A - \mu_B)\left(\frac{dX_A^s}{dX_A} - \frac{dX_A^l}{dX_A}\right). \tag{102}$$

If the boundary between liquid and solid were as shown in Fig. 22, then $X_A^s = X_A^l$ (the liquid and solid would have the same composition when in equilibrium at a point on the line $T_A T_B$). From eqn. (102)

$$(S^s - S^l)\frac{dT}{dX_A} = 0.$$

From eqn. (102)

$$(S^s - S^l)\,\frac{\mathrm{d}T}{\mathrm{d}X_A} = 0.$$

Since $S^s \neq S^l$, then $\mathrm{d}T/\mathrm{d}X_A = 0$. Thus the condition $X_A^s = X_A^l$ is only associated with $\mathrm{d}T/\mathrm{d}X_A = 0$, *i.e.* with a minimum or a maximum in the line $T_A T_B$ of Fig. 22. Except for this particular case therefore $X_A^s \neq X_A^l$. There is a difference between the composition of the liquid and solid phase in the general case.

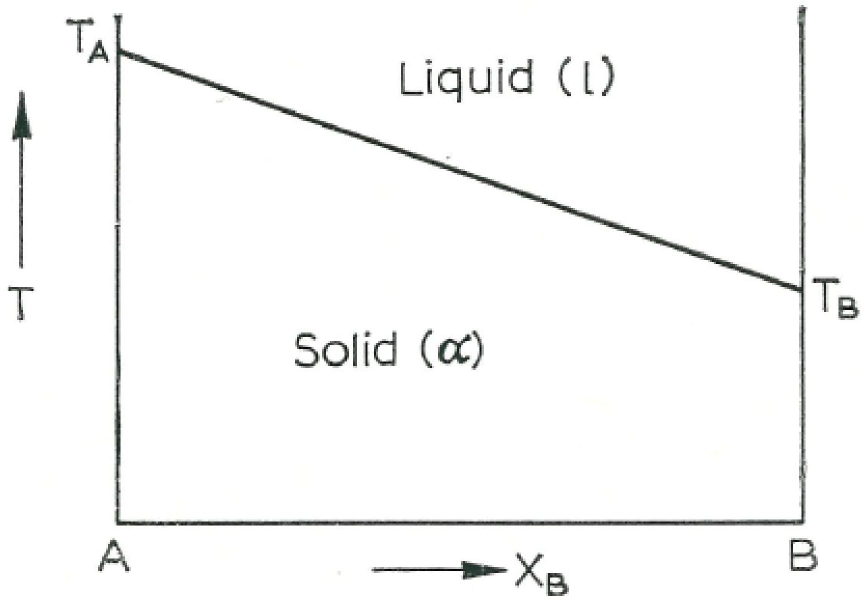

Fig. 22.

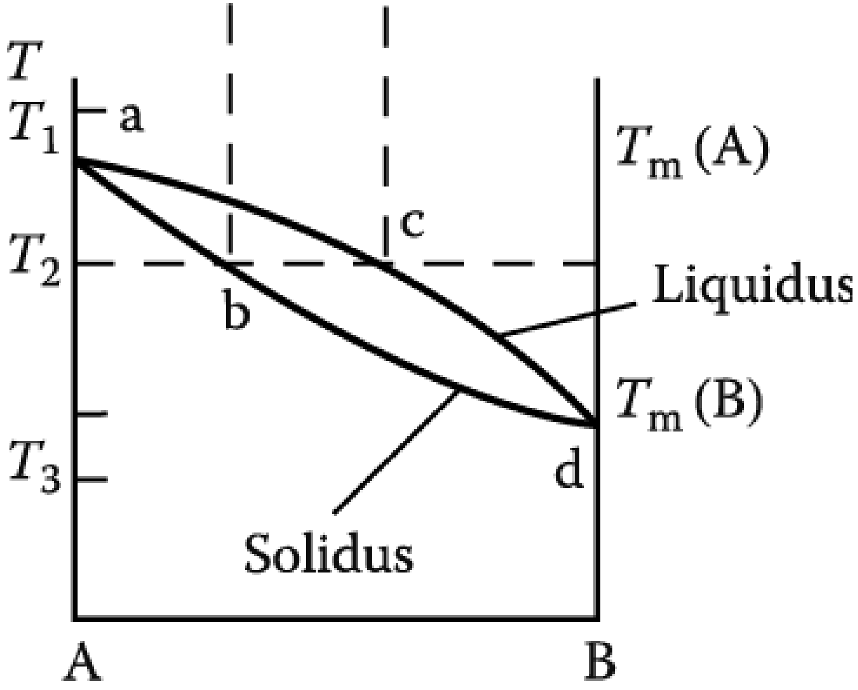

(f)

Assumption: a solute atom in a crystal requires either more or less energy to reach its active state than the atoms of the solvent.

*** If less, it is easier for solute atoms to "melt " than for solvent atoms, while it is equally easy for both to "freeze",**

Thus, equilibrium will be established when there are fewer solute atoms in the solid than in the liquid. → Figure 27 (a)

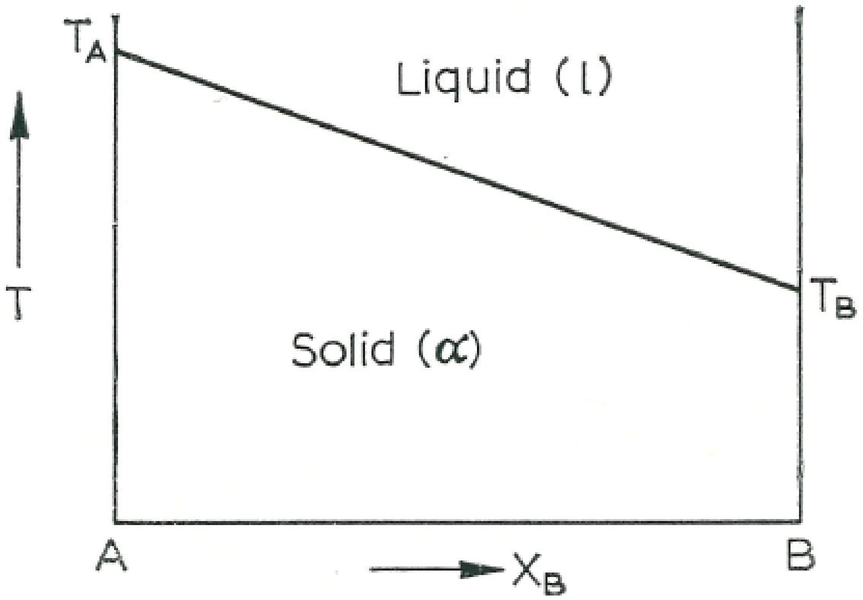

Fig. 22.

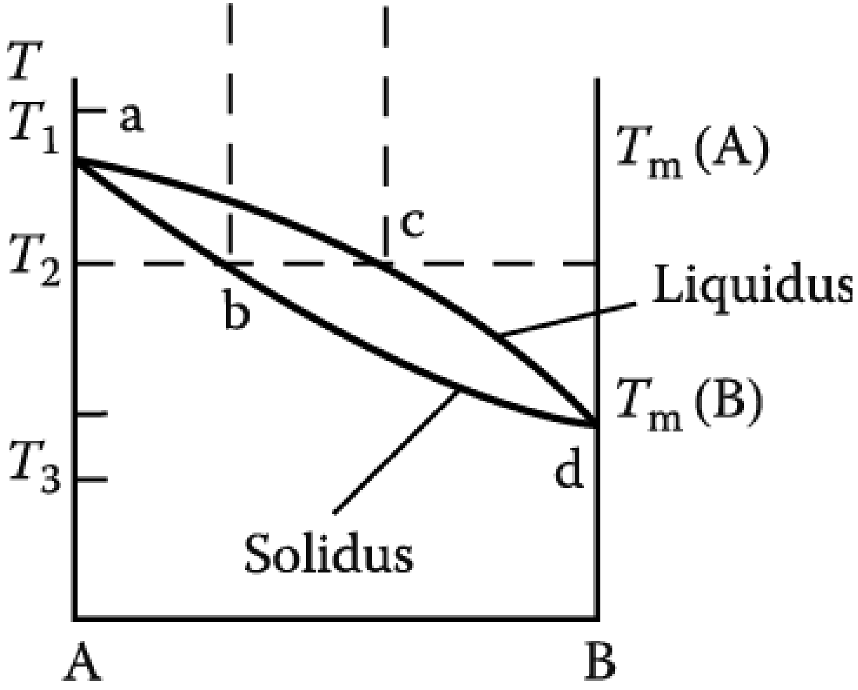

(f)

1) Simple Phase Diagrams

Assumption: (1) completely miscible in solid and liquid.

(2) Both are ideal soln.

$\Delta H^{L}_{mix} = 0 \quad \Delta H^{S}_{mix} = 0$

(3) $T_m(A) > T_m(B)$

(4) $T_1 > T_m(A) > T_2 > T_m(B) > T_3$

Draw G^L and G^S as a function of composition X_B at T_1, $T_m(A)$, T_2, $T_m(B)$, and T_3.

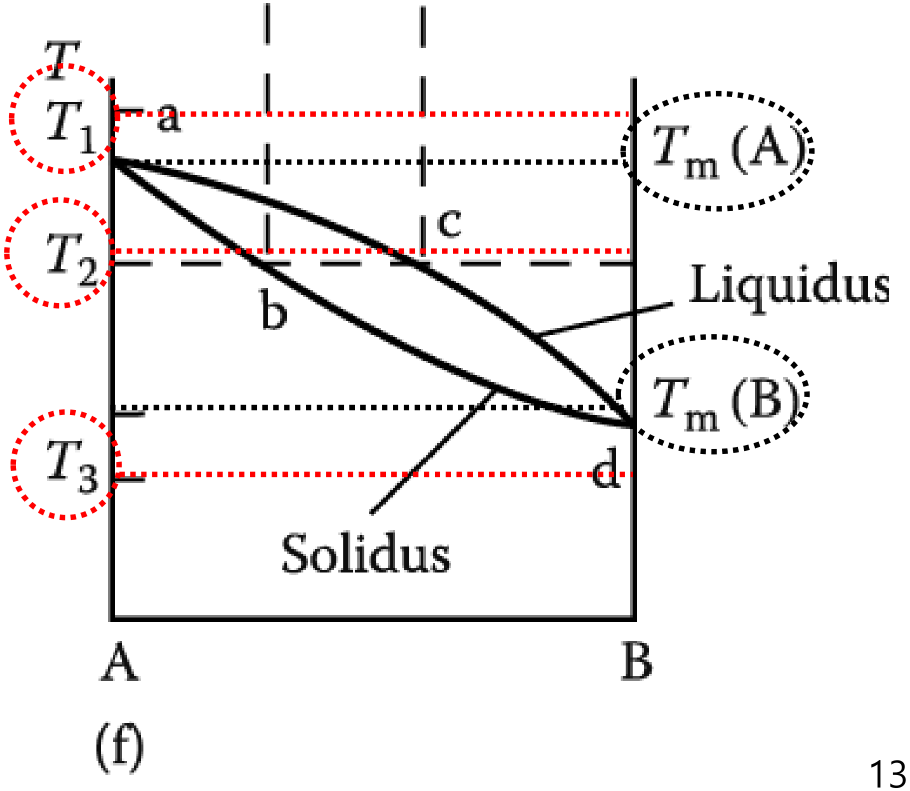

1.5 Binary phase diagrams

1) Simple Phase Diagrams

Assumption:

- **(1) completely miscible in solid and liquid.**
- **(2) Both are ideal soln.**
- **(3) $T_m(A) > T_m(B)$**
- **(4) $T_1 > T_m(A) > T_2 > T_m(B) > T_3$**

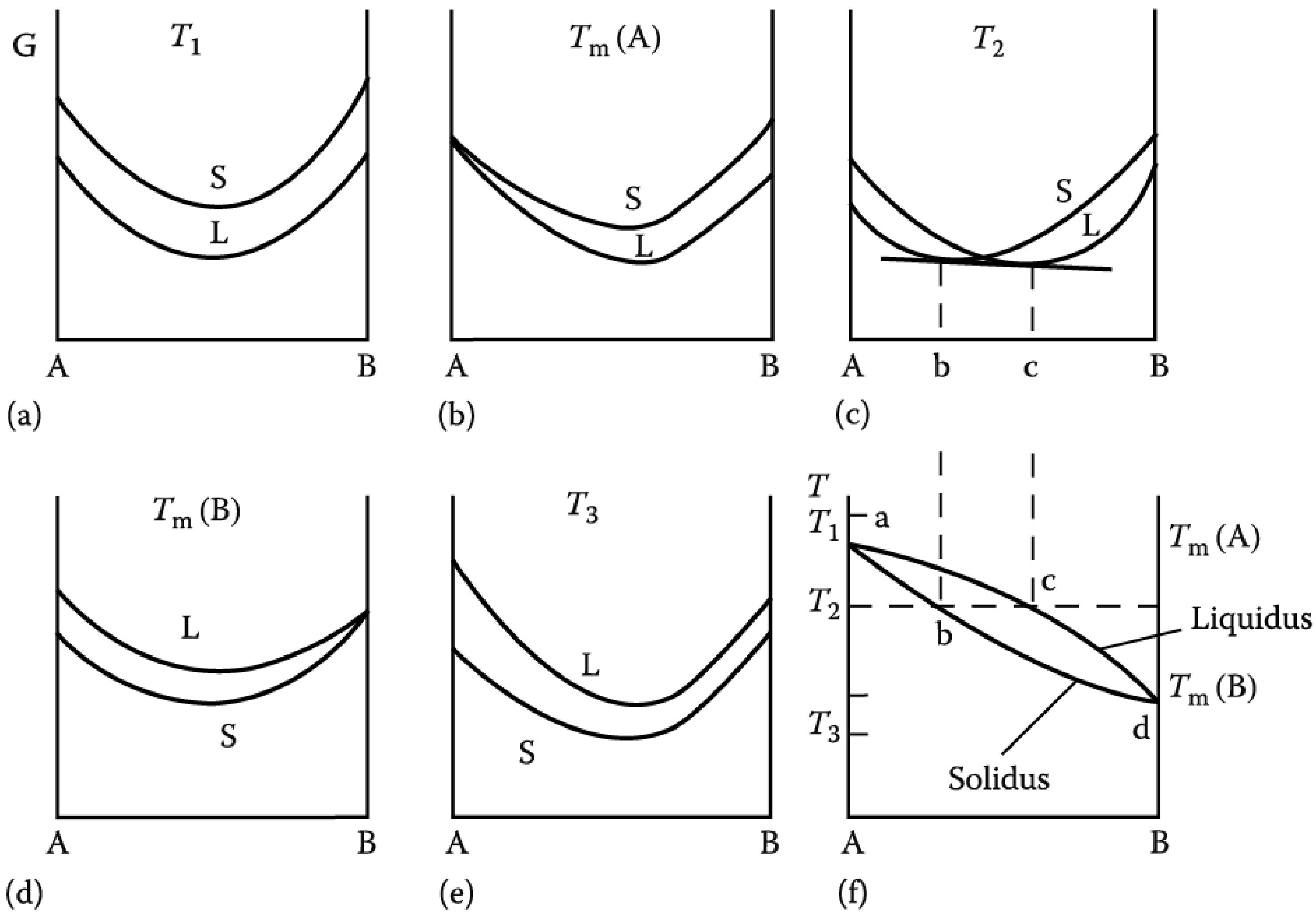

*** Consider actual (or so-called regular) solutions in which** $\Delta H_m \neq 0$, but $\Delta S_m = \Delta S_{m,\text{ideal}}$.

$$\Delta G_m^l = \Delta H_m^l + X_A^l \Delta G_A + RT(X_A^l \ln X_A^l + X_B^l \ln X_B^l).$$

Since

$$\Delta G_A = \Delta H_A - T\Delta S_A$$

then,

$$\underline{\Delta G_m^l = \Delta H_m^l + X_A^l \Delta H_A - X_A^l T\Delta S_A + RT(X_A^l \ln X_A^l + X_B^l \ln X_B^l).}$$

The free energy curve for the solid phase is:

$$\Delta G_m^s = \Delta H_m^s - X_B^s \Delta G_B + RT(X_A^s \ln X_A^s + X_B^s \ln X_B^s)$$

or,

$$\underline{\Delta G_m^s = \Delta H_m^s - X_B^s \Delta H_B + X_B^s T\Delta S_B + RT(X_A^s \ln X_A^s + X_B^s \ln X_B^s).}$$

1) Simple Phase Diagrams

a) Variation of temp.: $G^L > G^s$

b) T ↓ → Decrease of curvature of G curve

(∵ decrease of $-T\Delta S_{mix}$ effect)

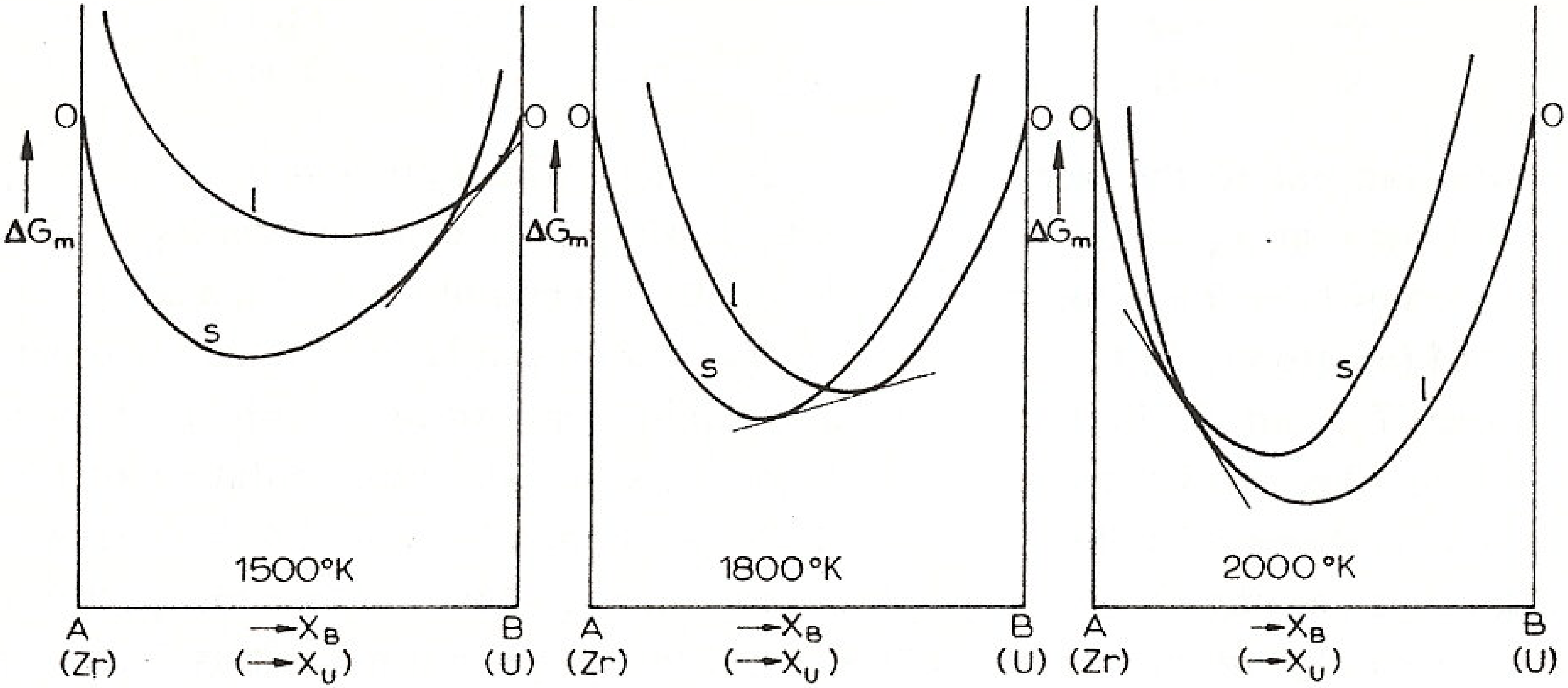

Fig. 26. Free energy curves for liquid and solid phases in the U–Zr system at 1500°, 1800° and 2000 °K.

It was assumed that $\Delta H_m^l = \Delta H_m^s$

1.5 Binary phase diagrams

1) Simple Phase Diagrams

a) Variation of temp.: $G^L > G^s$

b) T ↓ → Decrease of curvature of G curve

(∵ decrease of $-T\Delta S_{mix}$ effect)

Assumption:

(1) completely miscible in solid and liquid.

(2) Both are ideal soln.

(3) $T_m(A) > T_m(B)$

(4) $T_1 > T_m(A) > T_2 > T_m(B) > T_3$

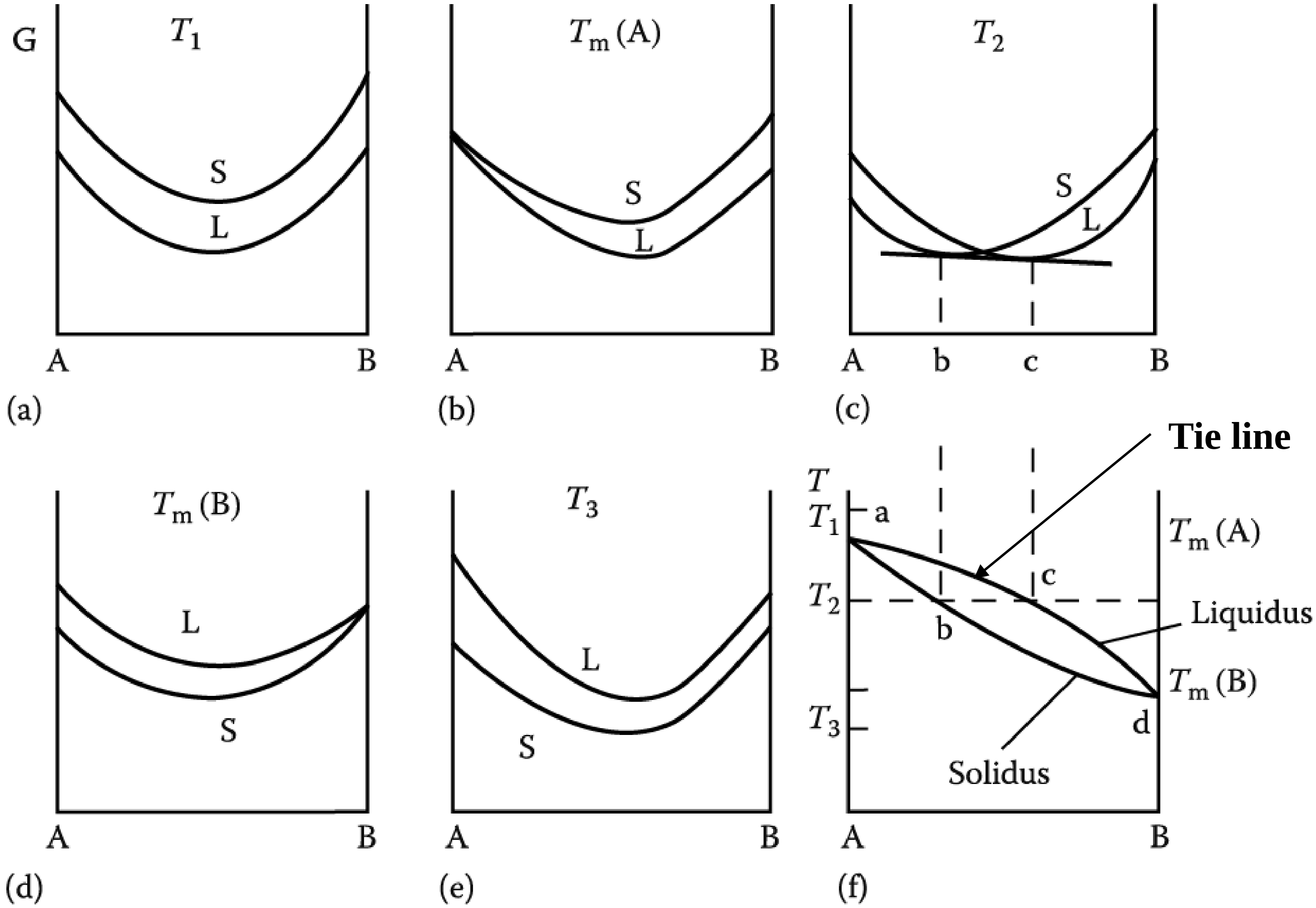

Referring to Fig. 23f, if A is regarded as the solvent, for very dilute solutions of B in A we can write

$$X_A \to 1 \quad \text{and} \quad -\ln X_A \simeq X_B.$$

In terms of eqn. (104):

$$X_A^l - X_A^s = \frac{\Delta H_A}{R}\left(\frac{T_A - T}{T T_A}\right).$$

Since $X_A^l = 1 - X_B^l$ and $X_A^s = 1 - X_B^s$

$$X_B^s - X_B^l = \frac{\Delta H_A}{R}\left(\frac{T_A - T}{T T_A}\right). \tag{105}$$

As T approaches T_A (in dilute solutions of B in solvent A), the denominator on the right-hand side of eqn. (105) can be written RT_A^2. Therefore

$$X_B^s - X_B^l = \frac{\Delta H_A}{RT_A^2}(T_A - T) \tag{106}$$

or,

$$\left(\frac{\mathrm{d}X_B^s}{\mathrm{d}T} - \frac{\mathrm{d}X_B^l}{\mathrm{d}T}\right)_{T=T_A} = \frac{\Delta H_A}{RT_A^2}. \tag{107}$$

Equations (106) and (107) are referred to as the Van't Hoff relation. They give the depression of the freezing point for a liquid solution in equilibrium with a solid solution. The difference in initial slopes of the solidus and liquidus curves, the slopes at $T = T_A$ and $X_A = 1$, are dependent on the latent heat of fusion of pure A (ΔH_A) but independent of the nature of the solute.

2) Variant of the simple phase diagram

$$\Delta H_{mix} > 0 \quad \Delta H^{\alpha}_{mix} > \Delta H^{l}_{mix}$$

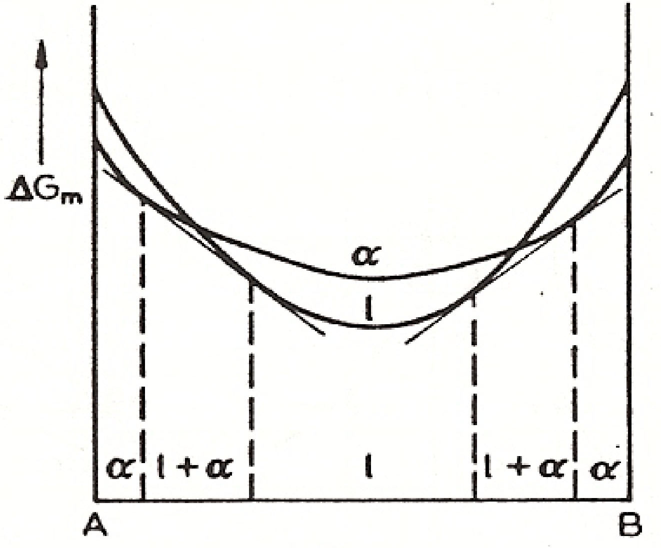

(a)

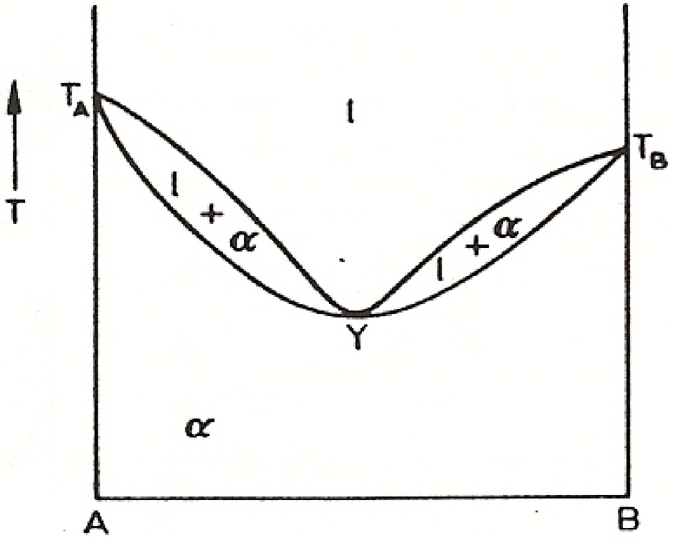

(b)

2) Variant of the simple phase diagram

$$\Delta H_{mix} > 0 \qquad \Delta H^{\alpha}_{mix} > \Delta H^{l}_{mix}$$

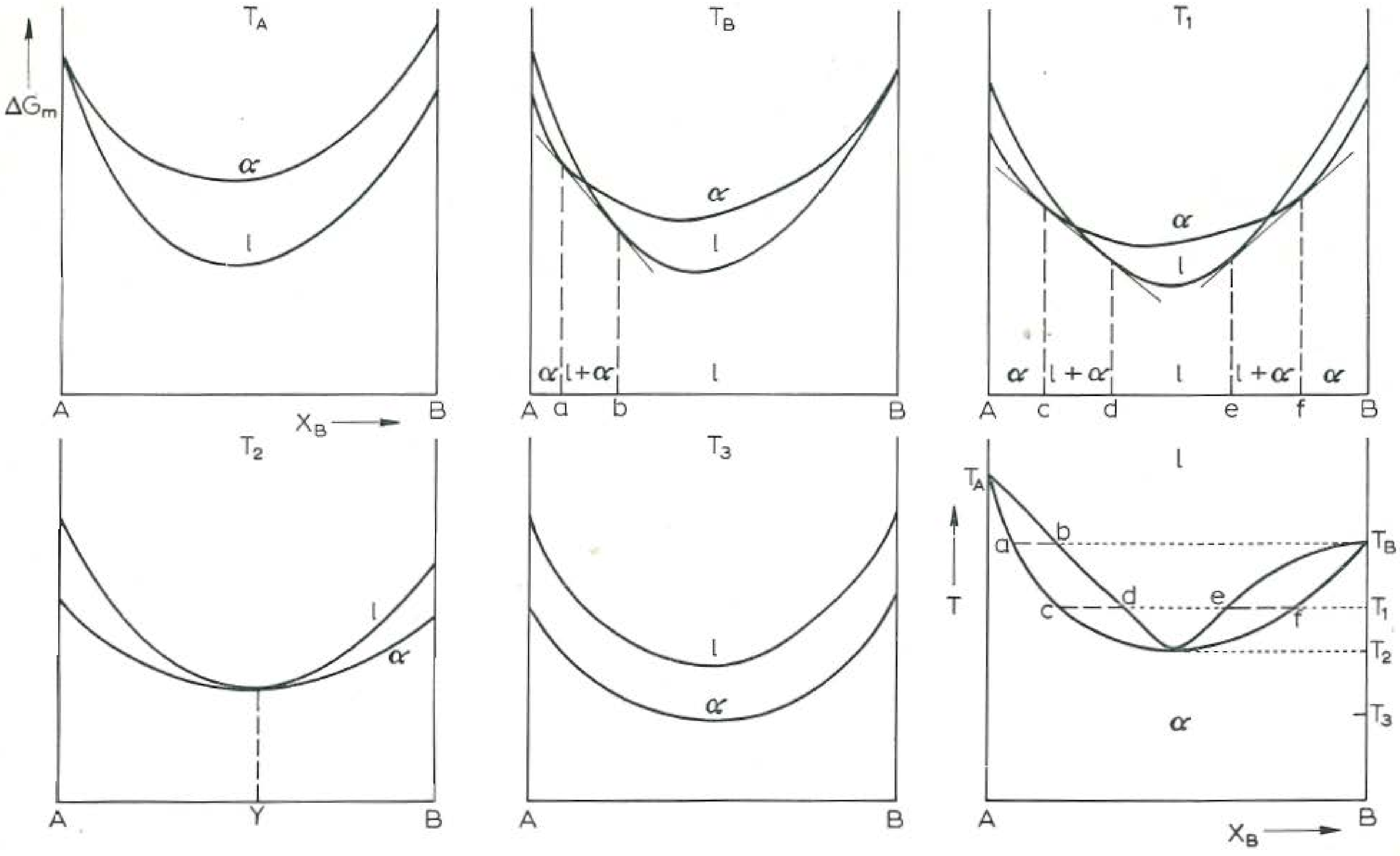

Fig. 30. Derivation of the phase diagram (Fig. 29b) from free energy curves for the liquid and solid phases. $T_A > T_B > T_1 > T_2 > T_3$.

2) Variant of the simple phase diagram

Systems with miscibility gab $\Delta H_{mix} > 0 \quad \Delta H^{\alpha}_{mix} > \Delta H^{l}_{mix}$

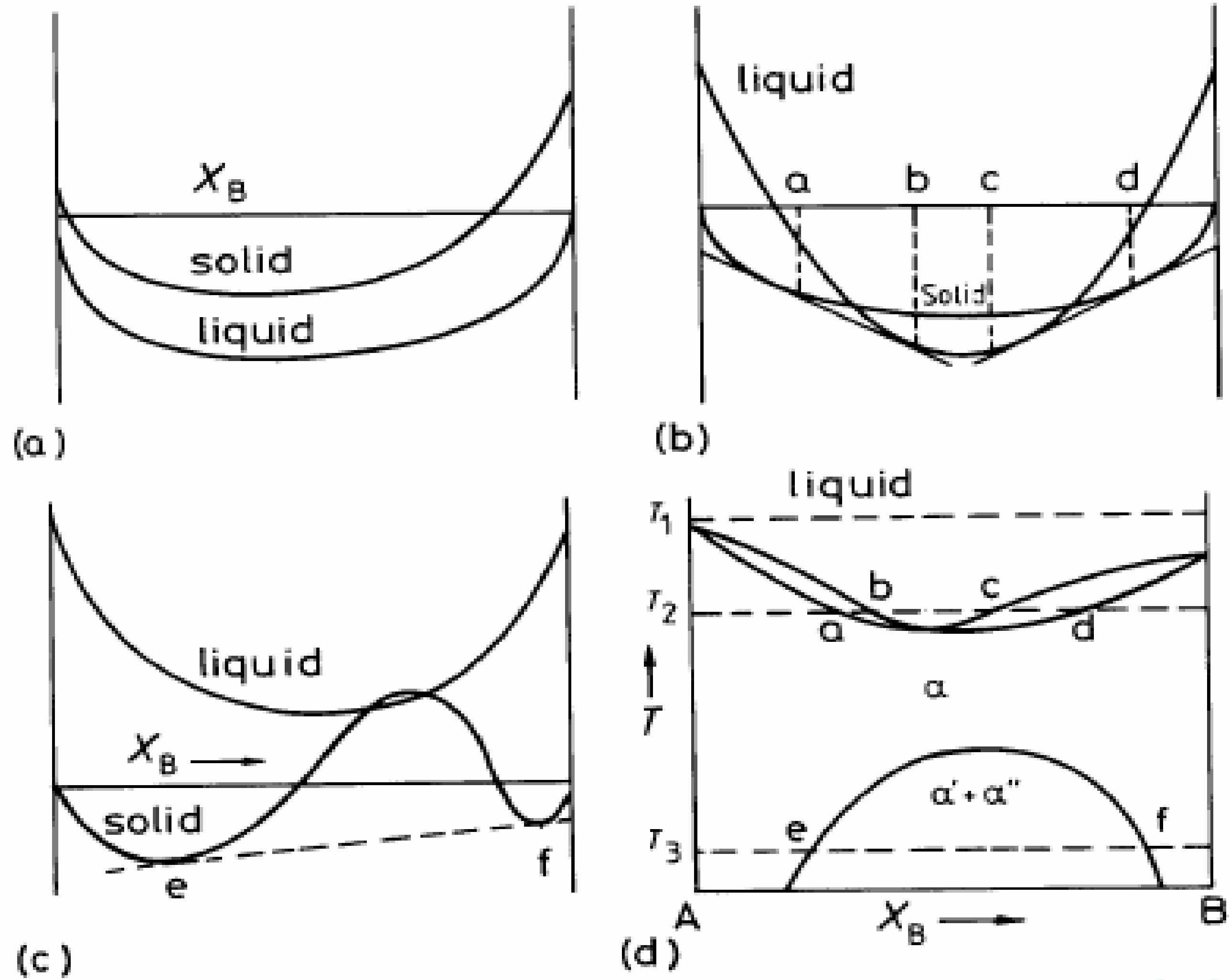

congruent minima

2) Variant of the simple phase diagram

$\Delta H_{mix} < 0$

$\Delta H^{\alpha}_{mix} < \Delta H^{l}_{mix} < 0$

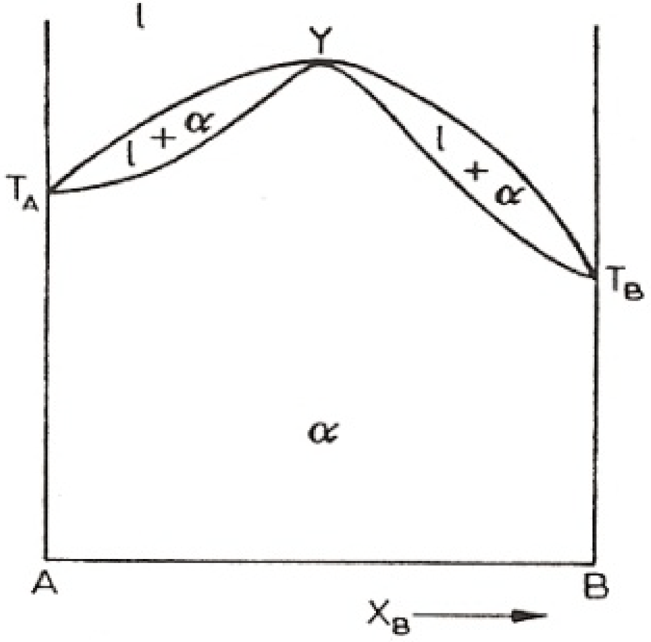

Fig. 32. Phase diagram with a maximum in the liquidus.

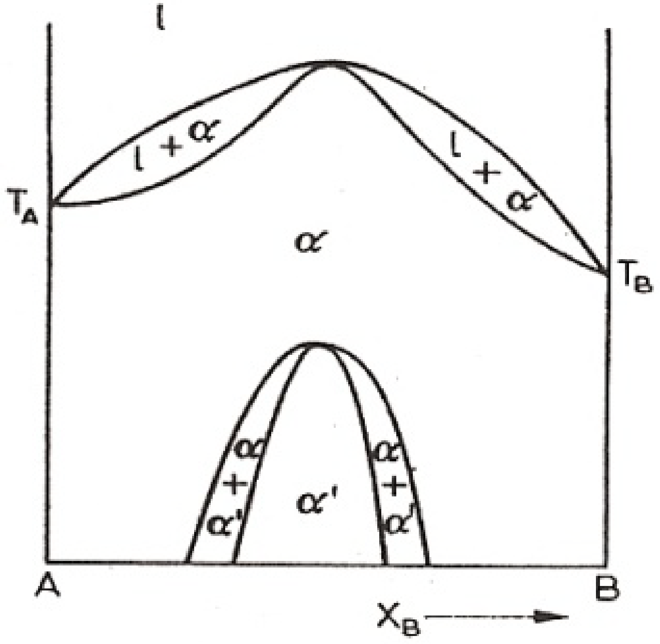

Fig. 33. Appearance of an ordered α′ phase at low temperatures.

Binary phase diagrams

1) Simple Phase Diagrams

Both are ideal soln. → At T change, curvature and width change of G curve by S

2) Systems with miscibility gap

$$\Delta H^{L}_{mix} = 0 \qquad \Delta H^{S}_{mix} > 0$$

At T change, curvature and width change of G curve by S + shape change of curve by H

4) Simple Eutectic Systems

$$\Delta H^{L}_{mix} = 0 \qquad \Delta H^{S}_{mix} >> 0$$

→ miscibility gap extends to the melting temperature.

3) Ordered Alloys

$$\Delta H^{L}_{mix} = 0 \qquad \Delta H^{S}_{mix} < 0$$

$\Delta H_{mix} < 0$ → A atoms and B atoms like each other. → Ordered alloy at low T

$\Delta H_{mix} << 0$ → The ordered state can extend to the melting temperature.

$$\boxed{\Delta H^{\alpha}_{mix} > \Delta H^{l}_{mix} > 0}$$

miscibility gab

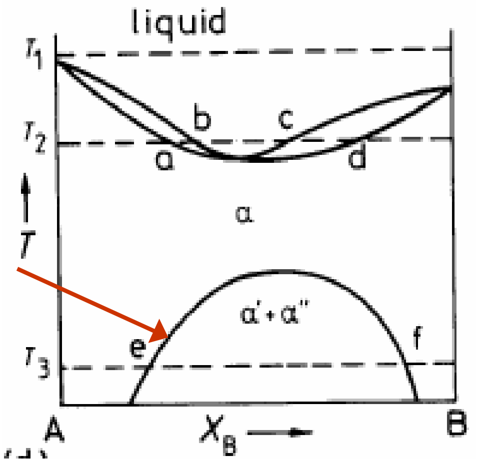

$$\boxed{\Delta H^{\alpha}_{mix} < \Delta H^{l}_{mix} < 0}$$

Ordered phase

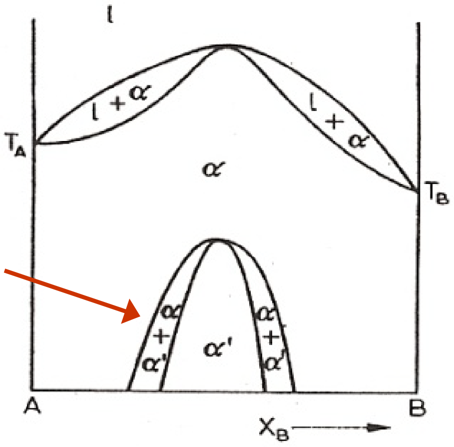

Eutectic reaction

Considerable difference between the melting points

$$\Delta H^{\alpha}_{mix} > \Delta H^{l}_{mix} > 0$$

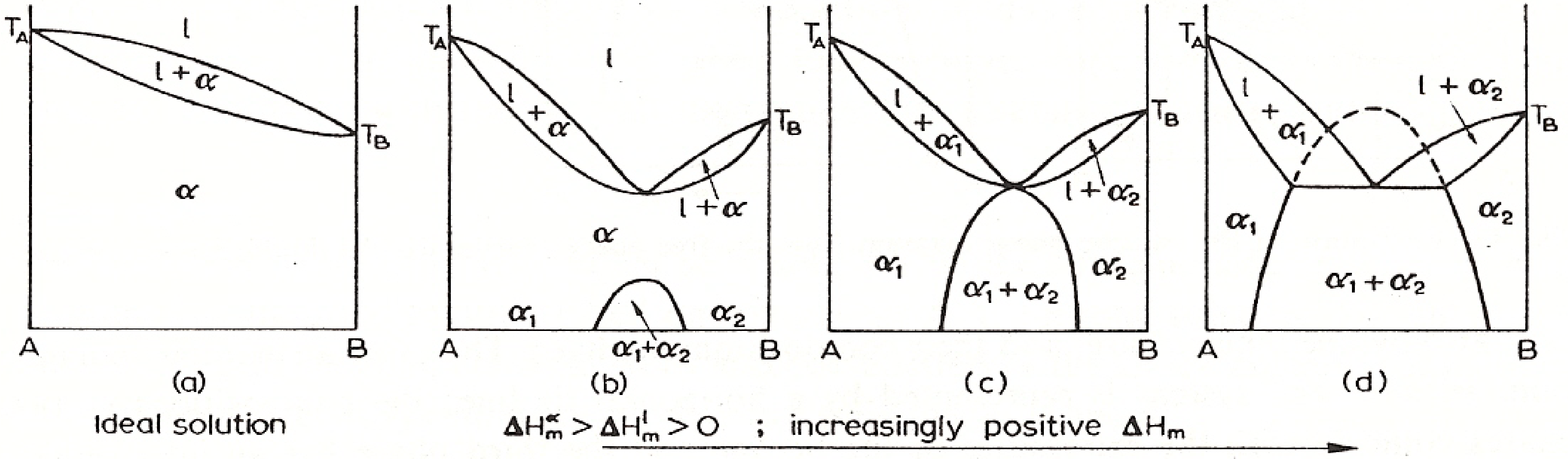

Fig. 43. Effect of increasingly positive departure from ideality in changing the phase diagram for a continuous series of solutions to a eutectic-type.

Peritectic reaction

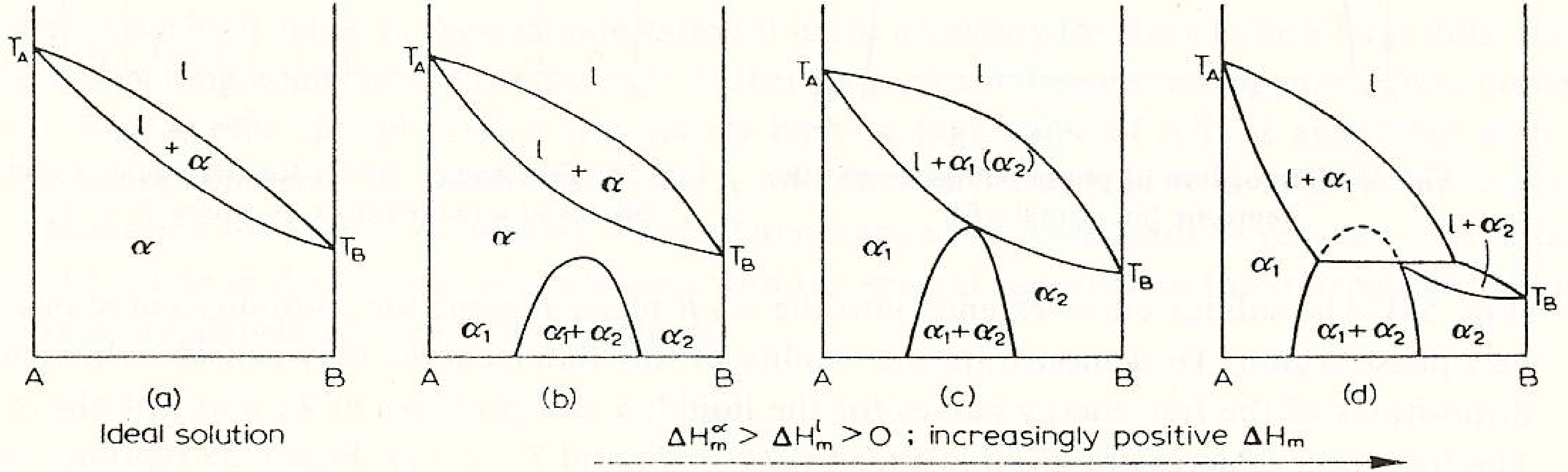

Fig. 61. Effect of increasingly positive departure from ideality in changing the phase diagram from a continuous series of solutions to a peritectic-type.

(a) Clustering

$\Delta H^{L}_{mix} = 0 \qquad \Delta H^{S}_{mix} > 0$

ε > 0, ΔH_{mix} > 0 / ΔH_{mix}~ +26 kJ/mol

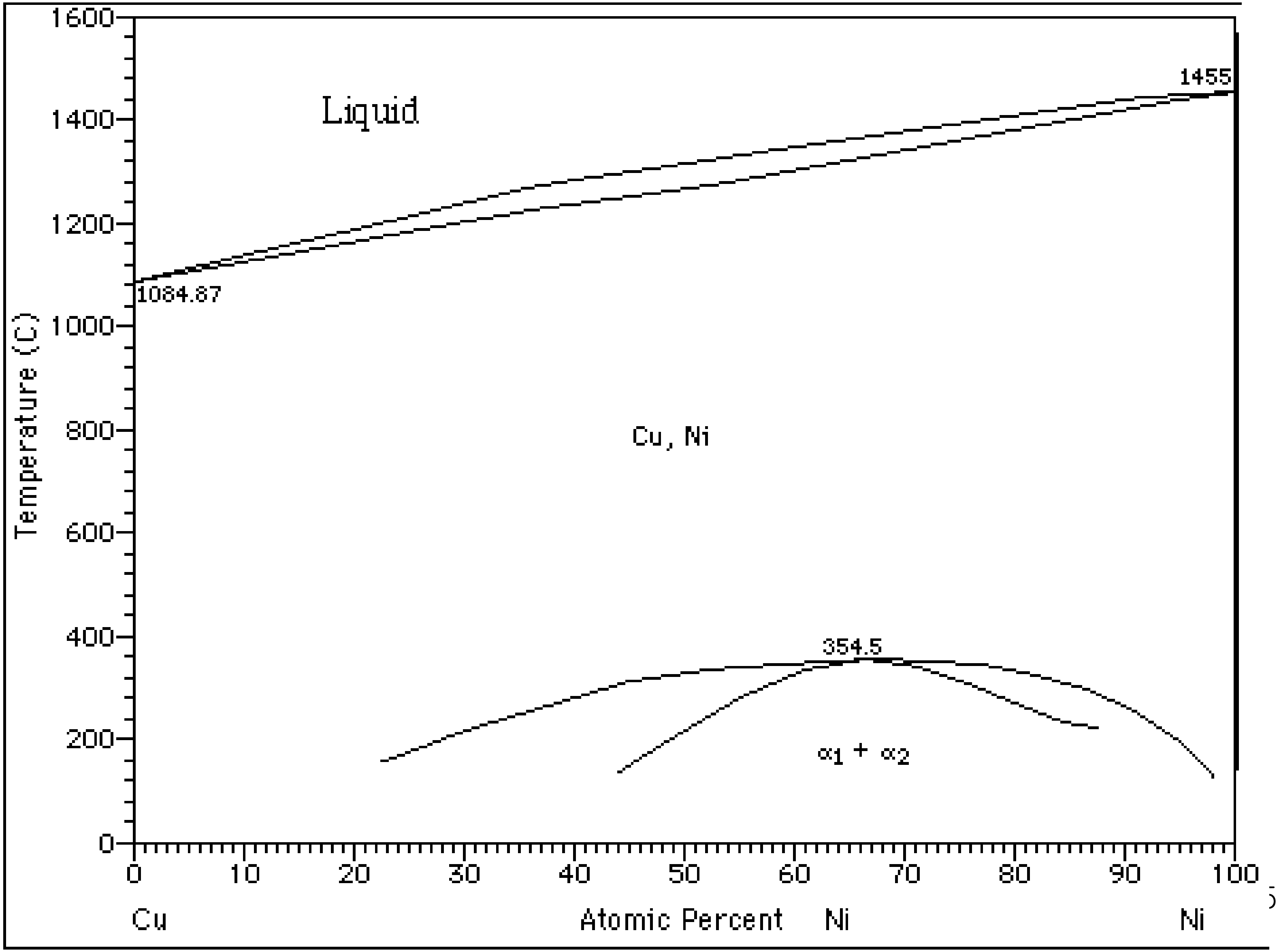

$\varepsilon > 0,\ \Delta H_{mix} > 0\ /\ \Delta H_{mix} \sim +5$ **kJ/mol**

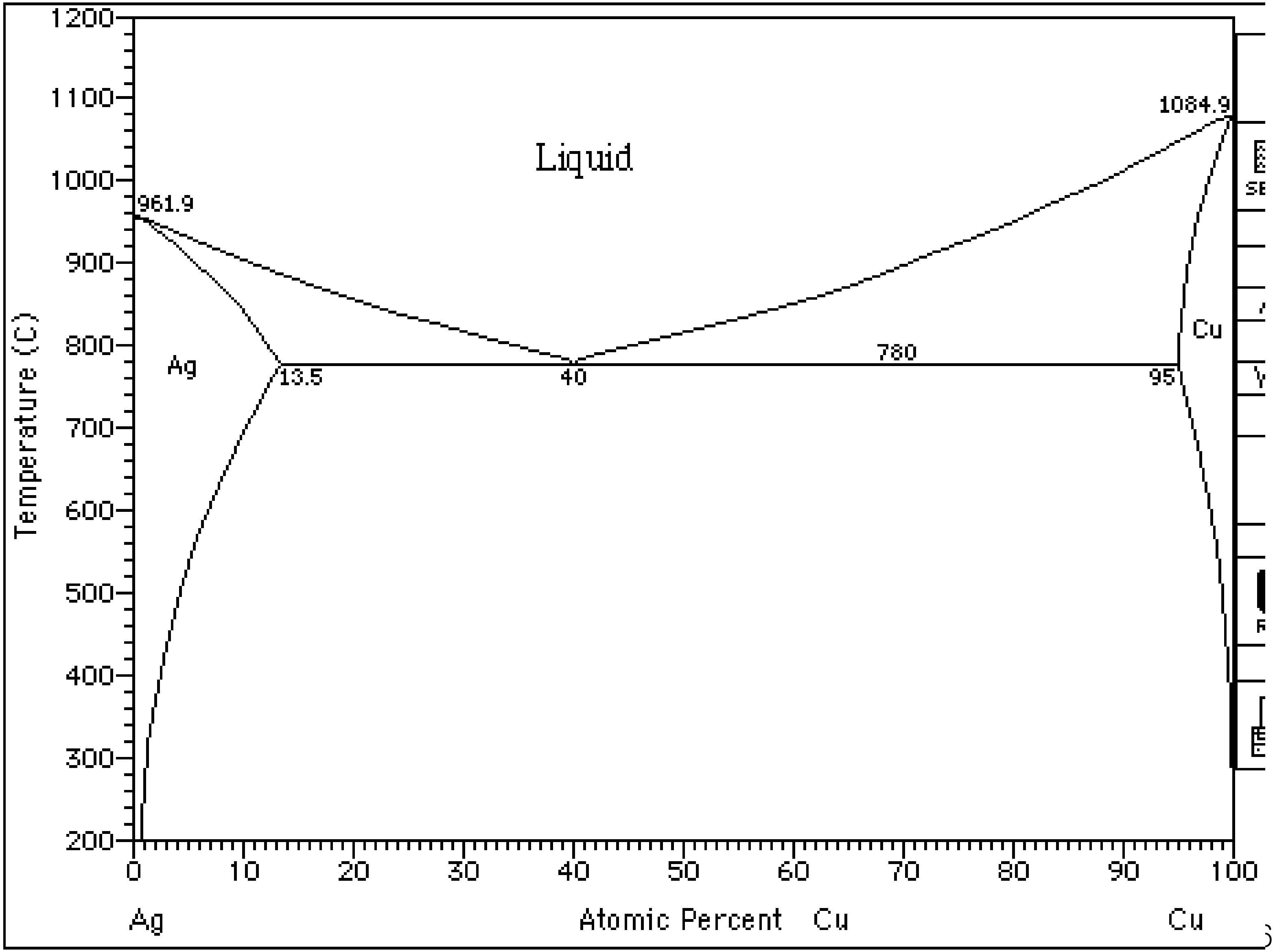

$\varepsilon >> 0$, $\Delta H_{mix} >> 0$ / $\Delta H_{mix} \sim +58$ kJ/mol

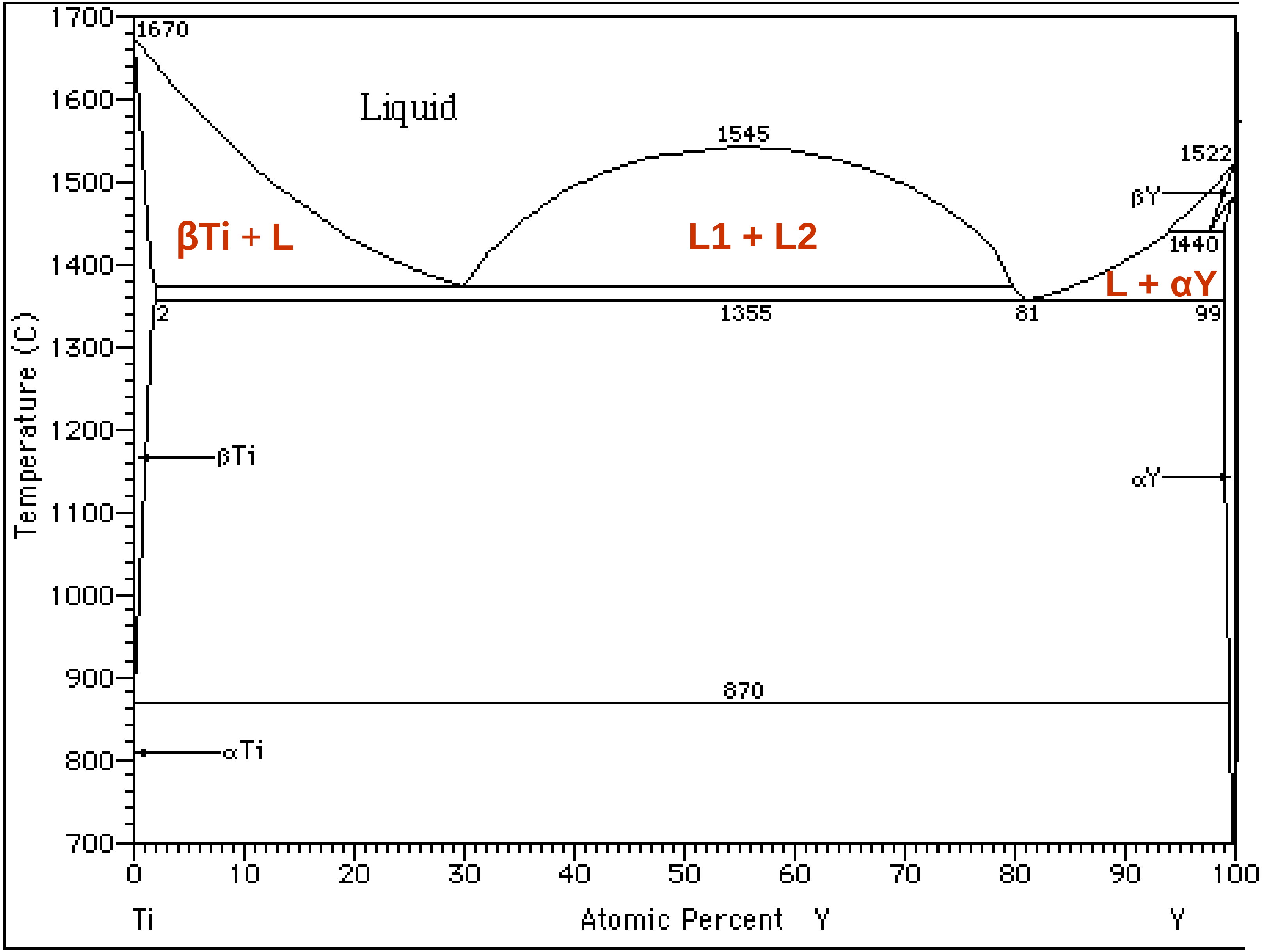

3) Ordered Alloys

$$\Delta H^{L}_{mix} = 0 \qquad \Delta H^{S}_{mix} < 0$$

$\Delta H_{mix} < 0$ → A atoms and B atoms like each other. → Ordered alloy at low T

$\Delta H_{mix} << 0$ → The ordered state can extend to the melting temperature.

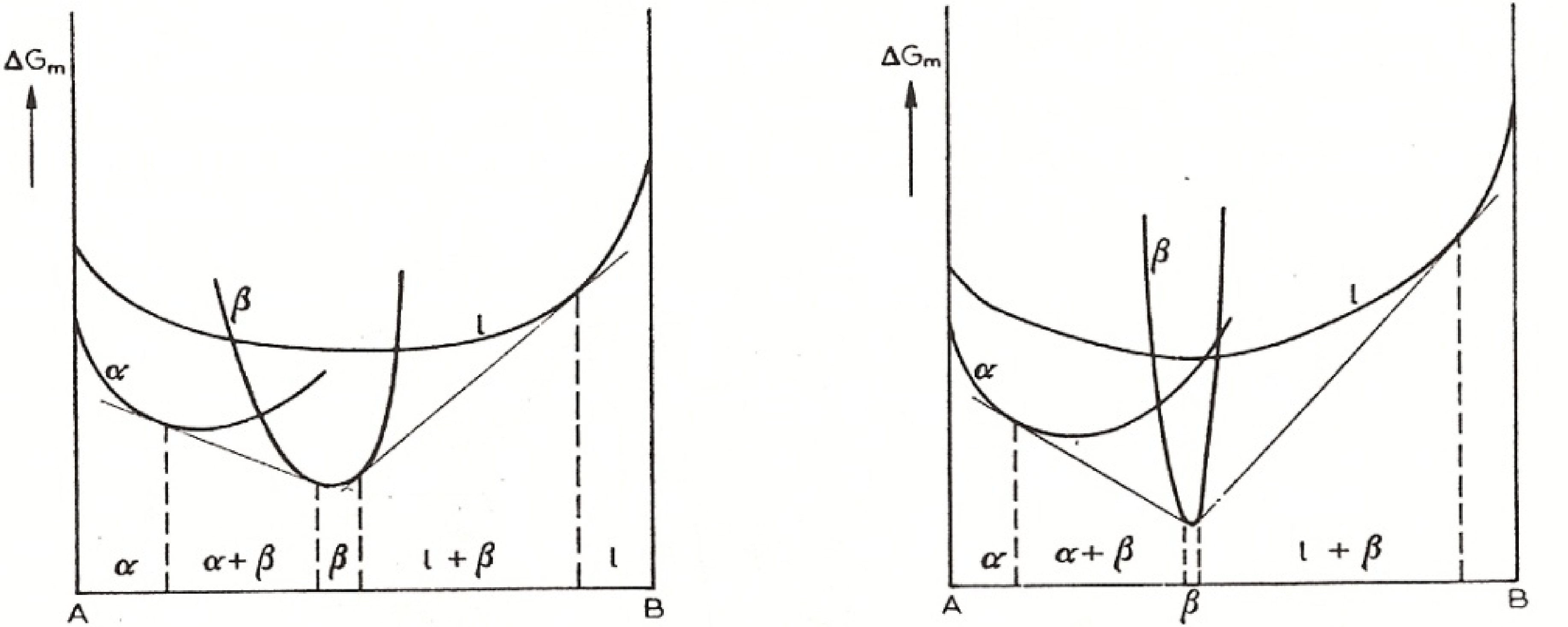

Fig. 70. Decreasing range of stability of an intermediate phase with its increasing stability relative to the termina solid solutions.

1.5 Binary phase diagrams

Intermediate Phase

*** Solid solution**

- → random mixing
- → entropy ↑
  negative enthalpy ↓

$$\boxed{\Delta H_{mix}^{S} < 0}$$

Wide compositional range
➔ G ↓

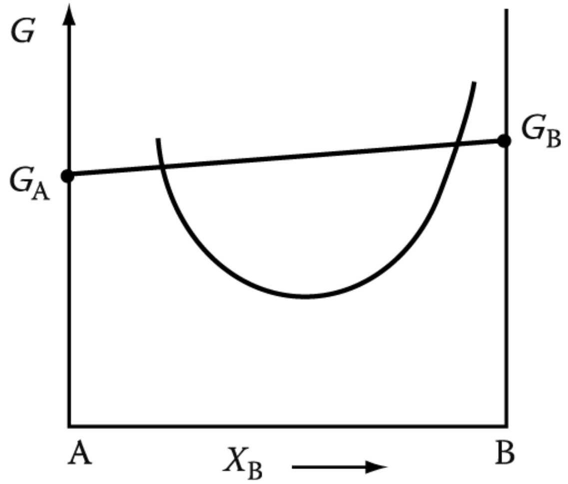

(b)

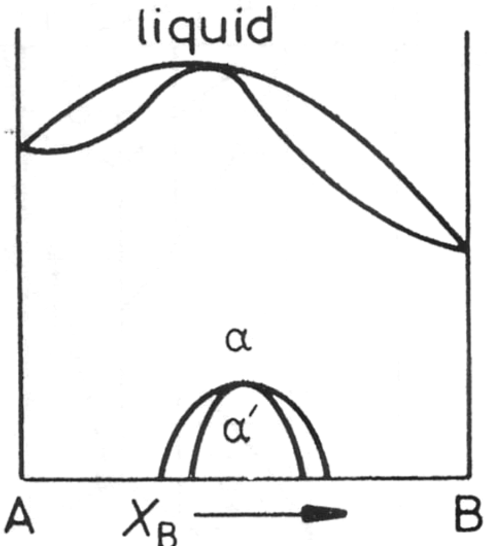

*** Compound : AB, A_2B…**

- → entropy↓
- → covalent, ionic contribution
- → enthalpy more negative ↓

$$\boxed{\Delta H_{mix}^{S} \ll 0}$$

Narrow compositional range
➔ G ↓

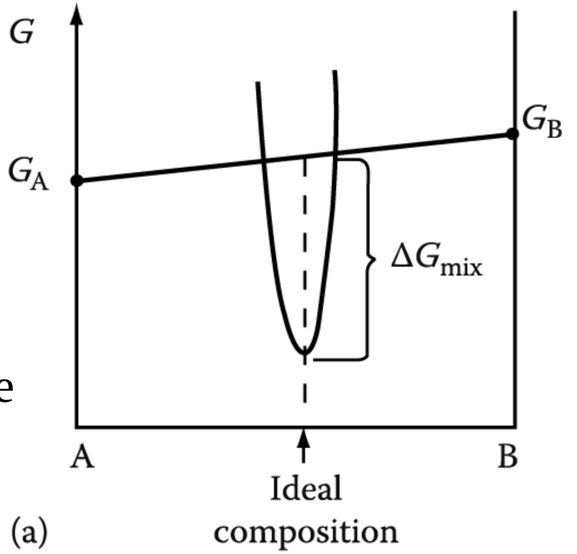

(a)

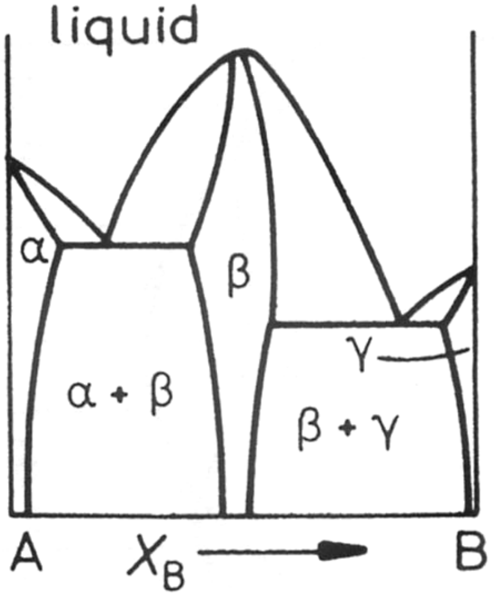

Ordered Phase

$\varepsilon < 0,\ \Delta H_{mix} < 0\ /\ \Delta H_{mix} \sim -20$ kJ/mol

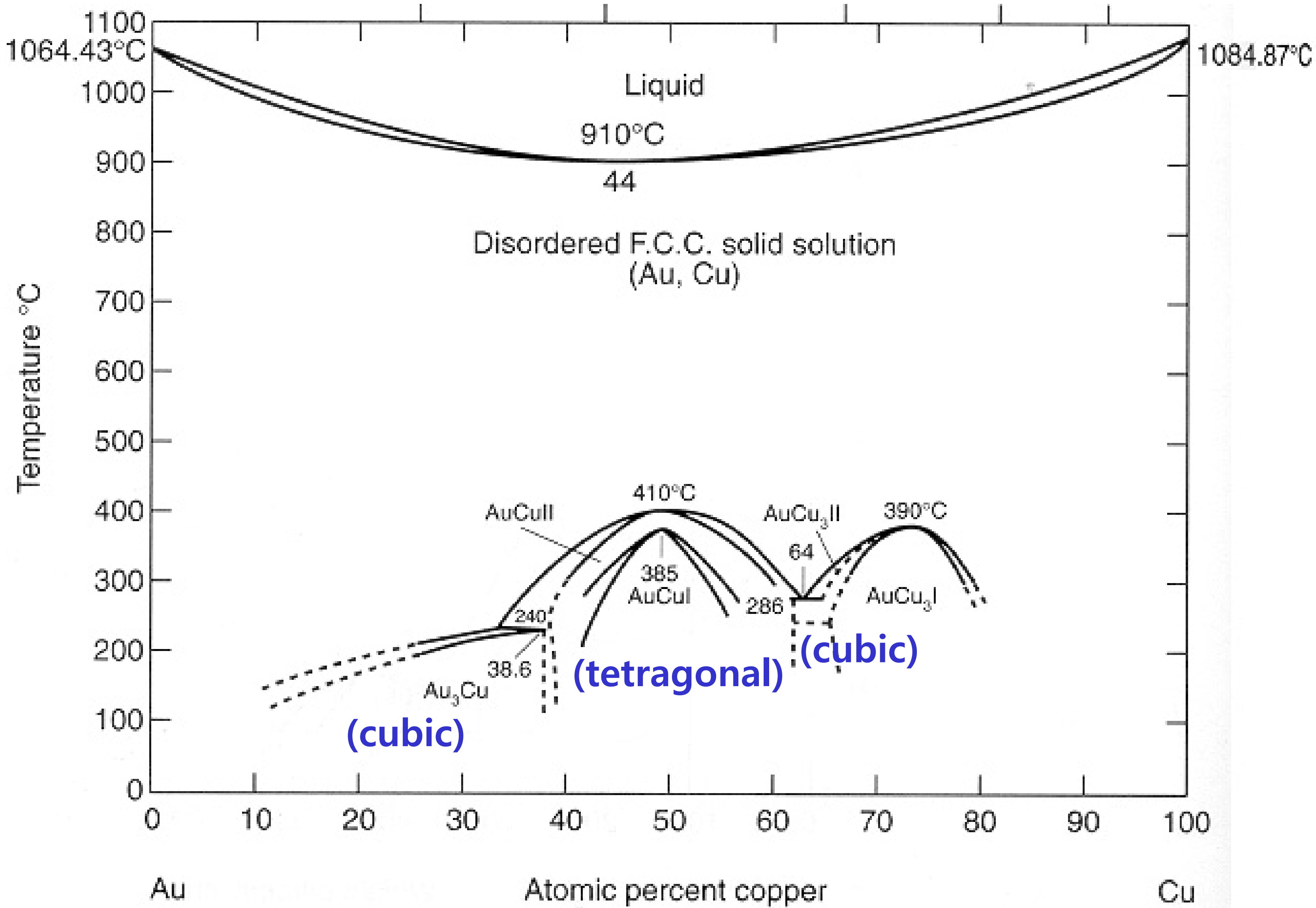

(tetragonal)

(cubic)

(cubic)

(fcc)

(complete solid solution)

(fcc)

Intermediate Phase

$\varepsilon < 0,\ \Delta H_{mix} < 0\ /\ \Delta H_{mix} \sim -21$ kJ/mol

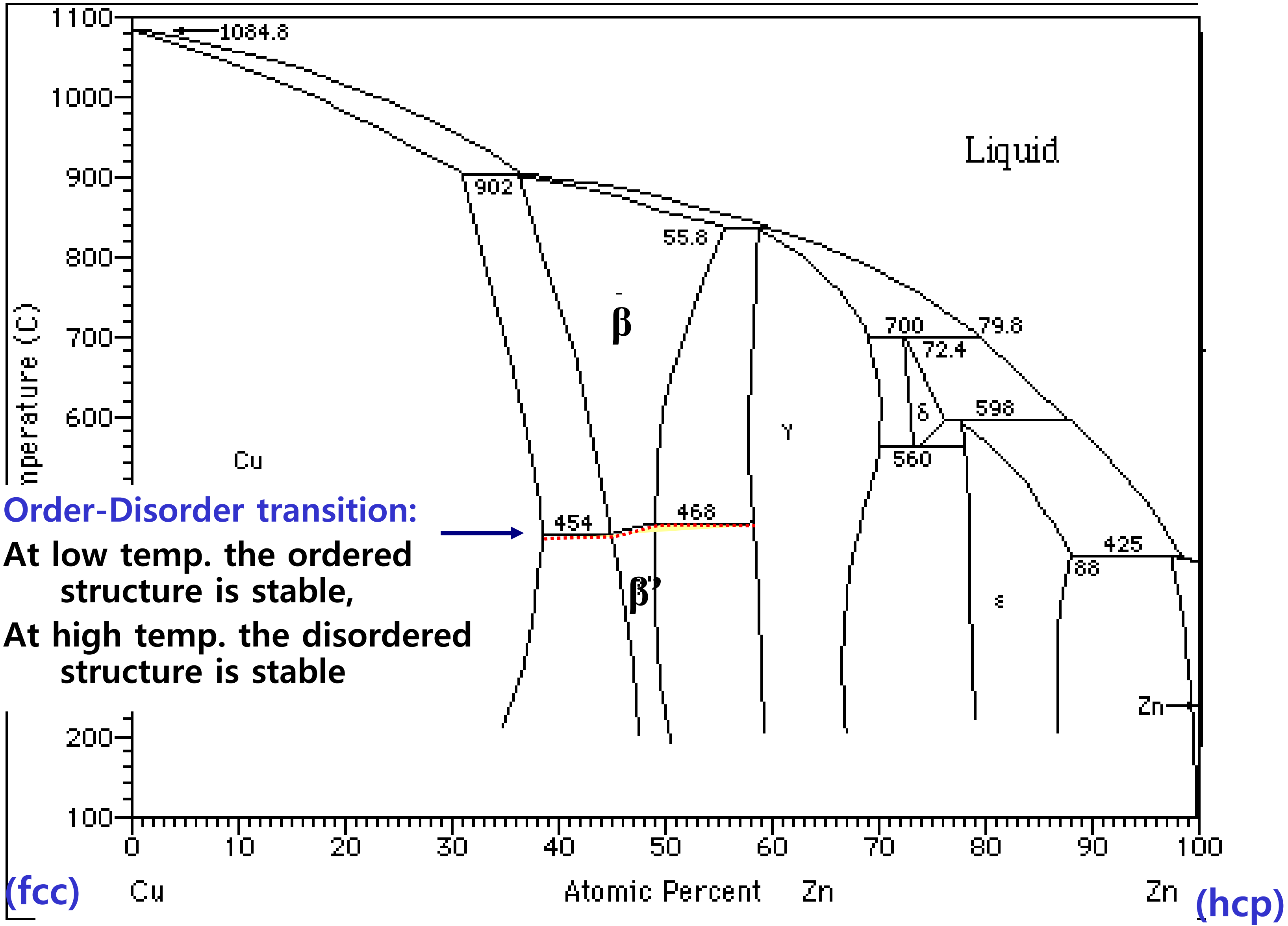

Order-Disorder transition:

At low temp. the ordered structure is stable,

At high temp. the disordered structure is stable

- α and η are terminal solid solutions
- β, β', γ, δ and ε are intermediate solid solutions.

Intermediate Phase

$\varepsilon < 0,\ \Delta H_{mix} < 0\ /\ \Delta H_{mix} \sim -38$ kJ/mol

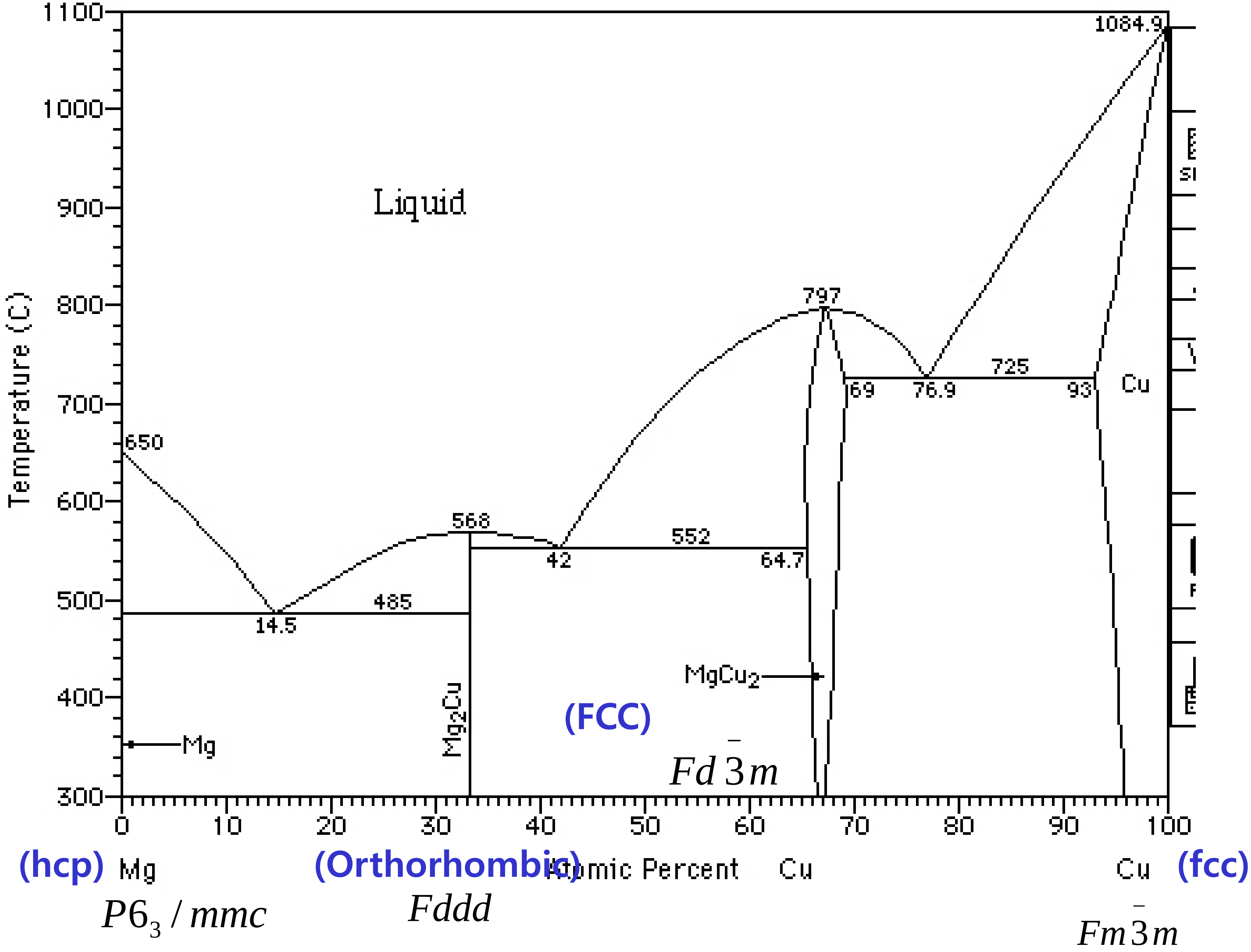

Intermediate Phase

$\varepsilon << 0$, $\Delta H_{mix} << 0$ / $\Delta H_{mix} \sim -142$ kJ/mol

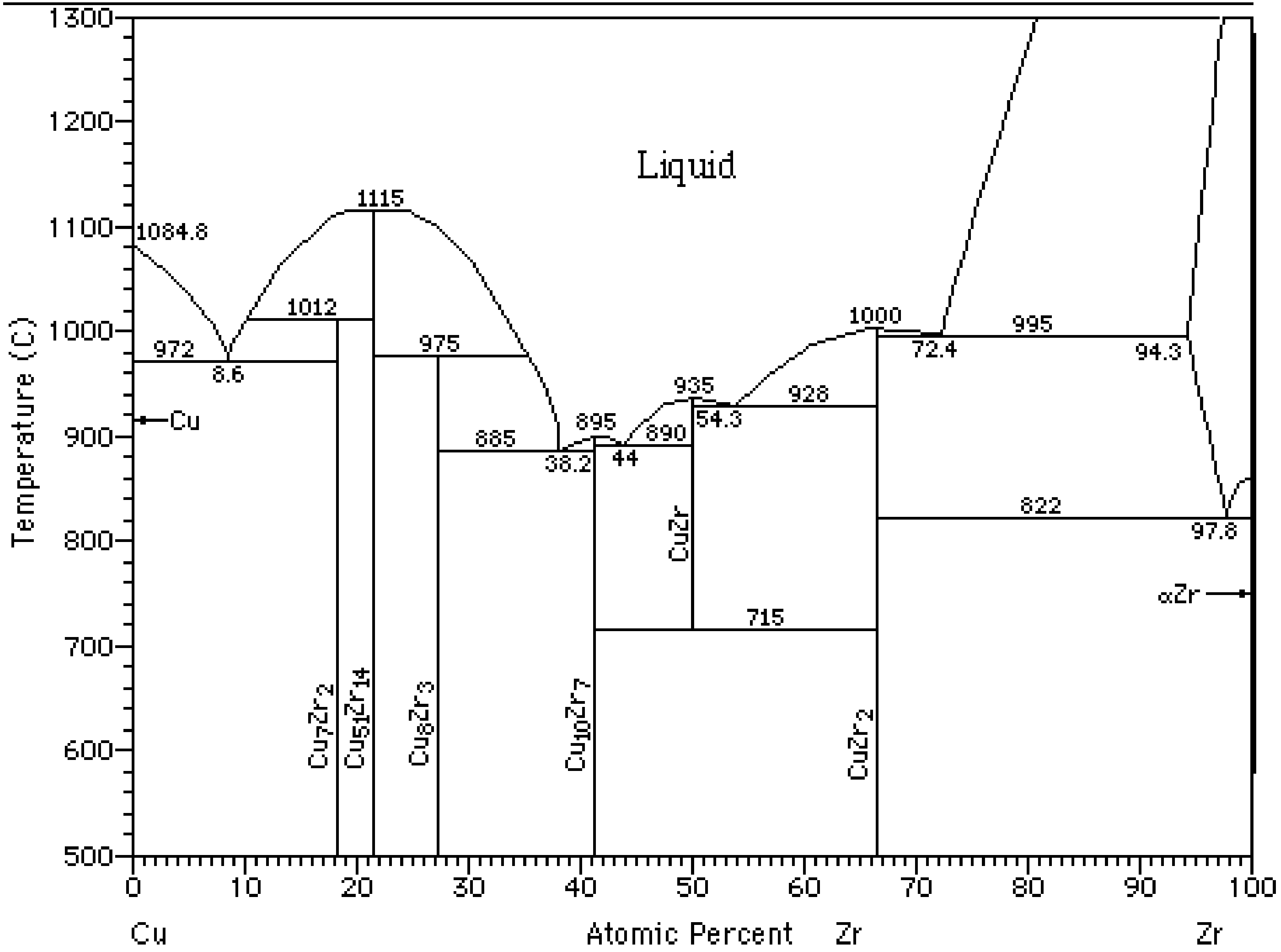

2.6 Origin of Defects

Microstructure is the collection of defects in the materials.

- ***Imperfection*** in Metallic Materials ;

  Point defect : Vacancies, interstitials, Impurities

  Line defect : Dislocations, Cellular and lineage substructure

  Plane defect : Grain Boundaries, Free Surfaces

  Bulk defect : Voids, Cracks

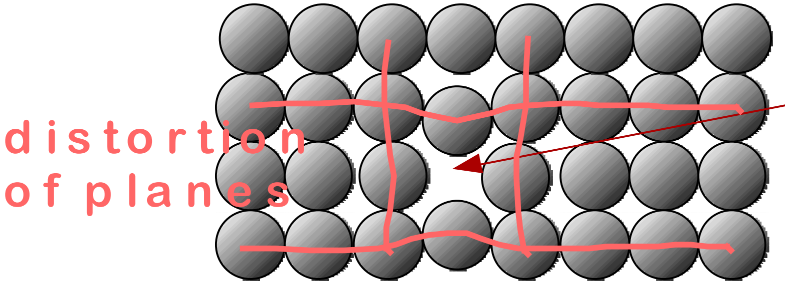

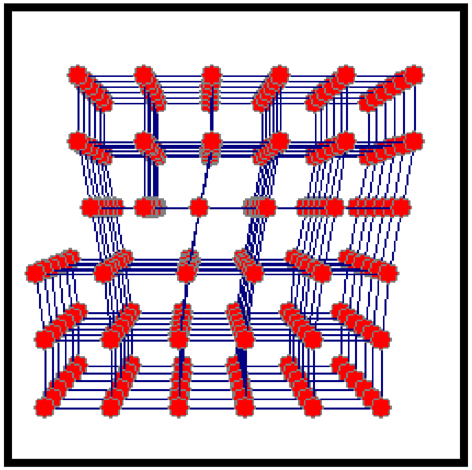

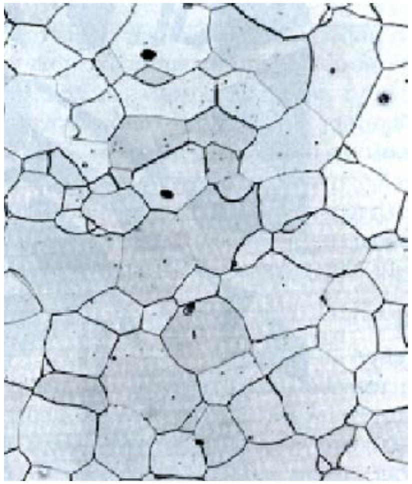

Heterogeneous Nucleation

Heterogeneous nucleation must occur on some substrate:

grain boundaries
triple junctions
dislocations
(existing) second phase particles

Consider a grain boundary: why is it effective?

Answer: by forming on a grain boundary, an embryo can offset its “cost” in interfacial energy by eliminating some grain boundary area.

1) Vacancy

a) Equilibrium Vacancy Concentration

$$\Delta G = \Delta H - T\Delta S$$

G of the alloy will depend on the concentration of vacancies and X_V^e will be that which gives the minimum free energy.

① **Vacancies increase the internal energy of crystalline metal due to broken bonds formation.** **(Here, vacancy-vacancy interactions are ignored.)**

$$\Delta H \cong \Delta H_V X_V$$

② **Vacancies increase entropy ("$\Delta G\downarrow$")** because they change the **thermal vibration frequency** and also the **configurational entropy**.

Small change due to changes in the vibrational frequencies

"Largest contribution"

- Total entropy change is thus

$$\Delta S = \Delta S_V X_V - R\{X_V \ln X_V + (1 - X_V)\ln(1 - X_V)\}$$

The molar free energy of the crystal containing X_V mol of vacancies

$$G = G_A + \Delta G = G_A + \Delta H_V X_V - T\Delta S_V X_V + RT\{X_V \ln X_V + (1 - X_V)\ln(1 - X_V)\}$$

➡ **With this information, estimate the equilibrium vacancy concentration.**

Equilibrium concentration X_V^e will be that which gives the minimum free energy.

at equilibrium $$\left(\frac{dG}{dX_V}\right)_{X_V = X_V^e} = 0$$

$$\Delta H_V - T\Delta S_V + RT \ln X_V^e = 0$$

A constant ~3, independent of T

Rapidly increases with increasing T

$$X_V^e = \boxed{\exp\frac{\Delta S_V}{R}} \cdot \exp\frac{-\Delta H_V}{RT}$$

putting $\Delta G_V = \Delta H_V - T\Delta S_V$

$$\boxed{X_V^e = \exp\frac{-\Delta G_V}{RT}}$$

- **In practice, ΔH_V is of the order of 1 eV per atom and X_V^e reaches a value of about 10^{-4}~10^{-3} at the melting point of the solid**

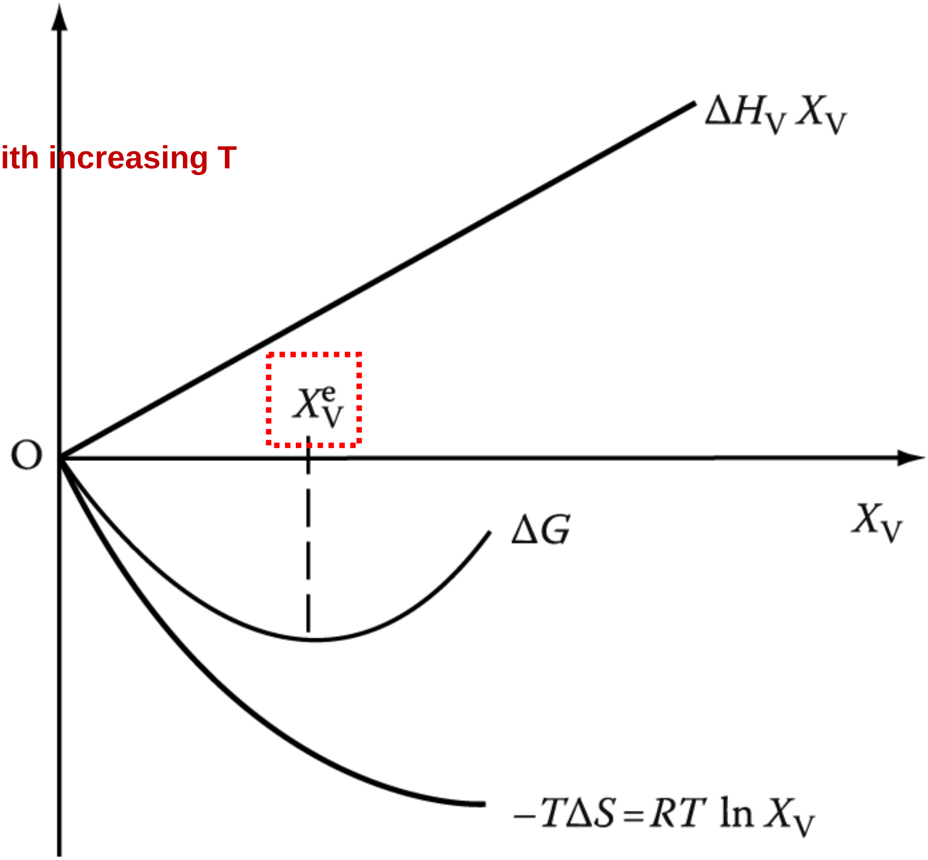

Fig. 1.37 Equilibrium vacancy concentration.

: adjust so as to reduce G to a minimum

Vacancies

- The role of vacancies is discussed in P&E and, essentially, dismissed in terms of heterogeneous nucleation sites.
- There is, however, an interesting and practical aspect of vacancies in nucleation that relates to diffusion.

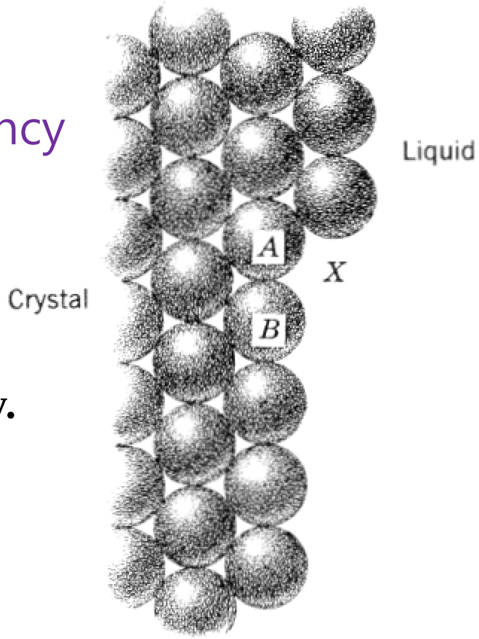

b) Formation of vacancies: Probability of creating a vacancy

$$P = \frac{\exp(-Q_D/RT)\ \text{: diffusive jump}}{\exp(-Q_F/RT)\ \text{: freezing process}} = 10^{-3}$$

Thus, one site in a thousand might be filled by the formation of a vacancy.

$$\boxed{C_V^{sol} - C_v^{eq.} = C_V^{excess}}$$

- Normally when you cool a material, the vacancy concentration changes only rather slowly from the high temperature value: quenching essentially preserves it.

→ With increasing time, vacancies disappeared through dislocation/ grain boundary/ interface.

c) Quenched-in Vacancies

In the vicinity of grain boundaries on subsequent aging,

Precipitate-Free Zone(PFZ) due to Vacancy Diffusion during quenching

Solute concentration within the zone ~ largely unchanged, but no precipitate at GB
∵ a critical vacancy supersaturation must be exceeded for nucleation to occur.

$$\boxed{X_V^e = \exp\frac{-\Delta G_V}{RT}}$$

$$T\uparrow \;\Rightarrow\; X_V^e \uparrow$$

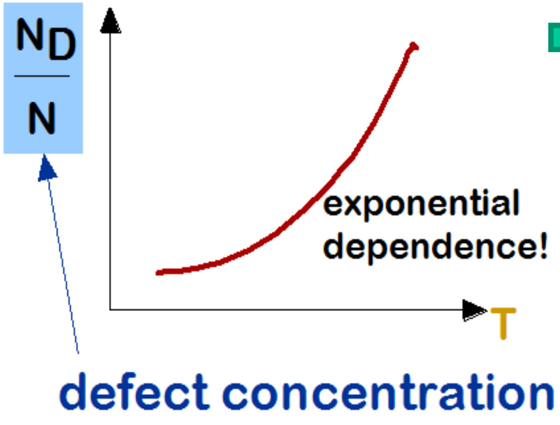

exponential dependence!

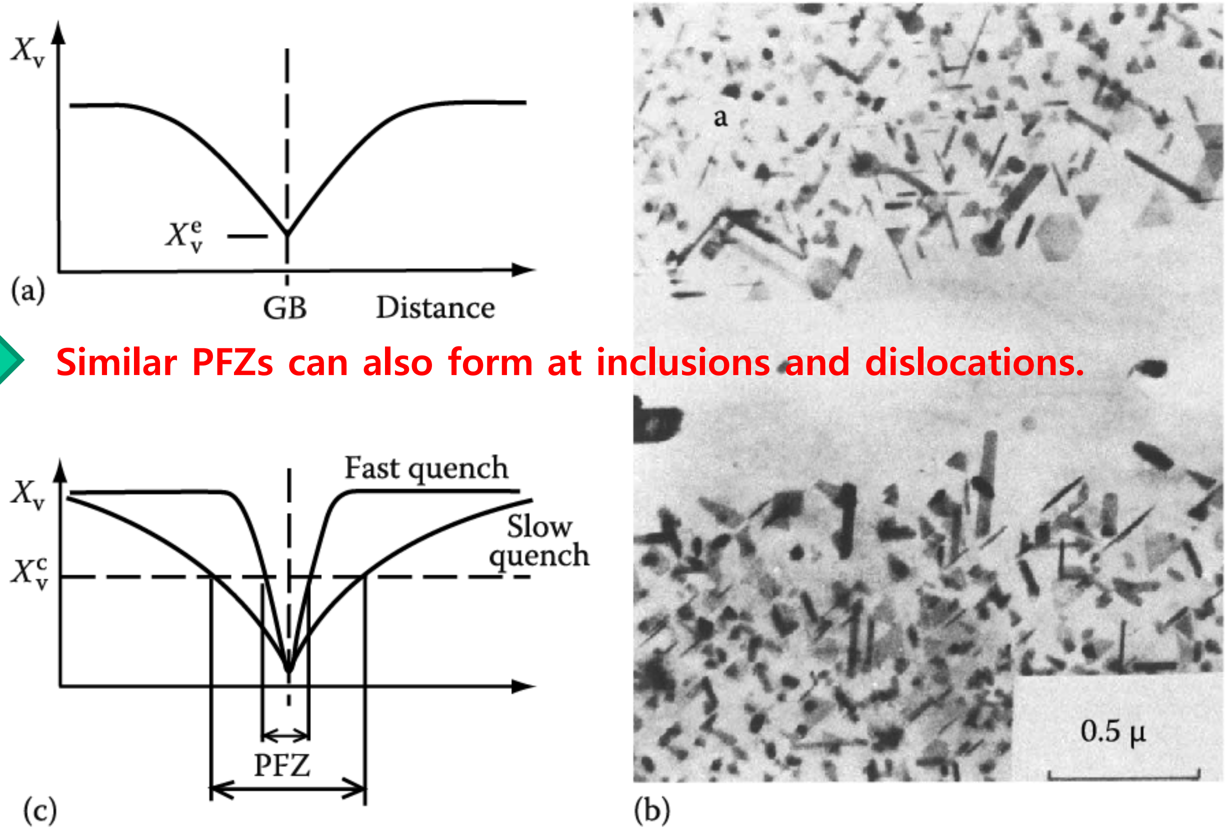

Similar PFZs can also form at inclusions and dislocations.

Fig. 5.35 A PFZ due to vacancy diffusion to a grain boundary during quenching.
(a) Vacancy concentration profile. (b) A PFZ in an Al-Ge alloy (x 20,000)
(c) Dependence of PFZ width on critical vacancy concentration X_v^c and rate of quenching.

d) Ways in which the resulting supersaturation of vacancies can decrease

① Grain boundaries and surfaces act as vacancy sinks

→ but, can drain vacancies only from a limited distance

(∵ **vacancy movement = random walk, $d \approx D_V \nu^{1/2} t^{1/2}$ (at const. temp.)**

→ The value of **d** depends on the rate of fall of temperature, but

d = between 0.01 cm and 0.1 cm. < smaller than effective radius of crystal

→ many of the vacancies must remain with in the grain.

② Dislocation may act as vacancy sinks

: edge dislocation climb → formation of jog → vacancy annihilation→ system G ↓

If surface, GB or dislocation sinks are not available within the diffusion distance imposed by the cooling rate.

③ Vacancies may precipitate by aggregation into a cluster,

which may take the form of a disc (either circular or related in shape to the symmetry of the crystal) or of a polyhedral void.

2) Dislocation

- ✓ are line defects,
- ✓ cause slip between crystal plane when they move,
- ✓ produce permanent (plastic) deformation.

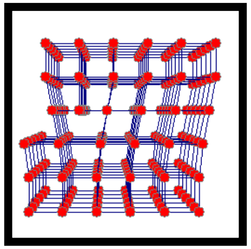

a) Formation mechanism of Dislocation

It is probable that there are a number of different ways in which dislocations may be introduced during crystal growth. Since dislocations are a non-equilibrium type of defect, they can be formed only as a result of non-equilibrium conditions during growth of the crystal.

① Externally applied stress.

→ A small stress is sufficient to increase the dislocation content of a crystal to an enormous extent, but that the generation of dislocations where non were present cannot take place as a result of the application of a stress unless there is a very severe stress concentration.

② Stress of thermal origin.

: Formation of thermal shock/ Materials with differential contraction (i.e. crystal and oxide)/ Polycrystalline specimen of a material that has different thermal expansion characteristics in different crystallographic directions→ High stress via thermal origin : relief by the motion and multiplication of dislocations

③ Concentration gradients

: high local concentration gradient → stress ↑ → Formation of dislocation → G of system↓ (Assumption: the crystal grows by the propagation of platelets or steps across its surface)

But, metals solidify by normal growth rather than by lateral propagation of steps.

(Exception: to permit cellular or dendritic solidification or changes of rate of solidification cause "banding" (see chapter 5)

④ Condensation of vacancies → **Collapse of a disc of vacancies**

→ Collapse of a disc of vacancies = 1) a ring of partial dislocation surrounding a disc of stacking fault or 2) a ring of complete dislocation with no stacking fault

→ **Limitation:** a) **supersaturation of vacancies should not be sufficient to cause discs to form spontaneously until the temperature had fallen far below the melting point (i.e. 147 ℃ for Al (T_m=660 ℃), 382 ℃ for Cu (T_m=1083 ℃)) /**
b) Collapse can occur when vacancy disc's radius exceeds about 5 interatomic spacings

→ **If dislocation ring has formed, it can grow by climb.**
If it is a ring of complete dislocation, it can move by slip.

⑤ Stresses due to inclusions. (dislocation density ~ inclusion density)

Coherency Loss

Precipitates with coherent interfaces = low interfacial E + coherency strain E

Precipitates with non-coherent interfaces = higher interfacial E

$$\Delta G(coherent) = 4\mu\delta^2 \cdot \frac{4}{3}\pi \boxed{r^3} + 4\pi \boxed{r^2} \cdot \gamma_{ch} \Leftrightarrow \Delta G(non-coherent) = 4\pi \boxed{r^2} \cdot (\gamma_{ch} + \gamma_{st})$$

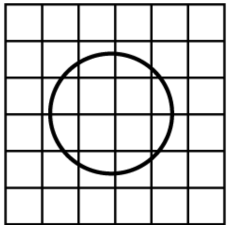

Coherency strain energy
Eq. 3.39

Chemical interfacial E

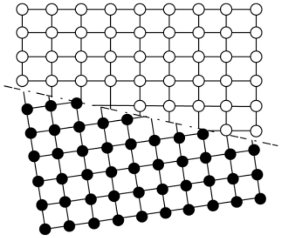

Chemical and structural interfacial E

$$\frac{4}{3}\pi r^3 \left(4\pi\mu\delta^2\right) + 4\pi r^2 \left(\gamma_{ch}\right) = 4\pi r^2 \left(\gamma_{st} + \gamma_{ch}\right)$$

coherent

ΔG_s-relaxed

$$\therefore \boxed{r_{crit} = \frac{3 \cdot \gamma_{st}}{4\mu\delta^2}}$$

$$\approx \frac{1}{\delta}$$

($\delta = (d_\beta - d_\alpha)/ d_\alpha$: misfit)

$$for\ small\ \delta, \quad \gamma_{st} \propto \delta$$

(semicoherent interface)

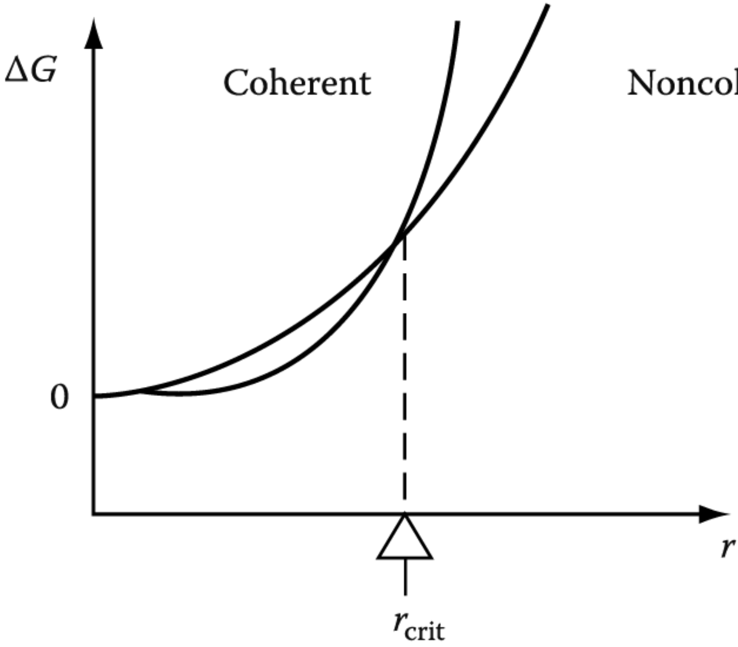

Fig. 3. 52 The total energy of matrix + precipitate vs. precipitate radius for spherical coherent and non-coherent (semicoherent of incoherent) precipitates.

⑥ Growth error: inherent feature

3) Lineage structure: An imperfection structure characterizing a crystal, parts of which have slight differences in orientation

→ often observed in crystals grown from the melt are arrays of dislocations that originated by the condensation of vacancies and subsequent collapse of the discs to form dislocation loos. (sub-boundary)

* lineage structure in Al → originates as a "river type" structure

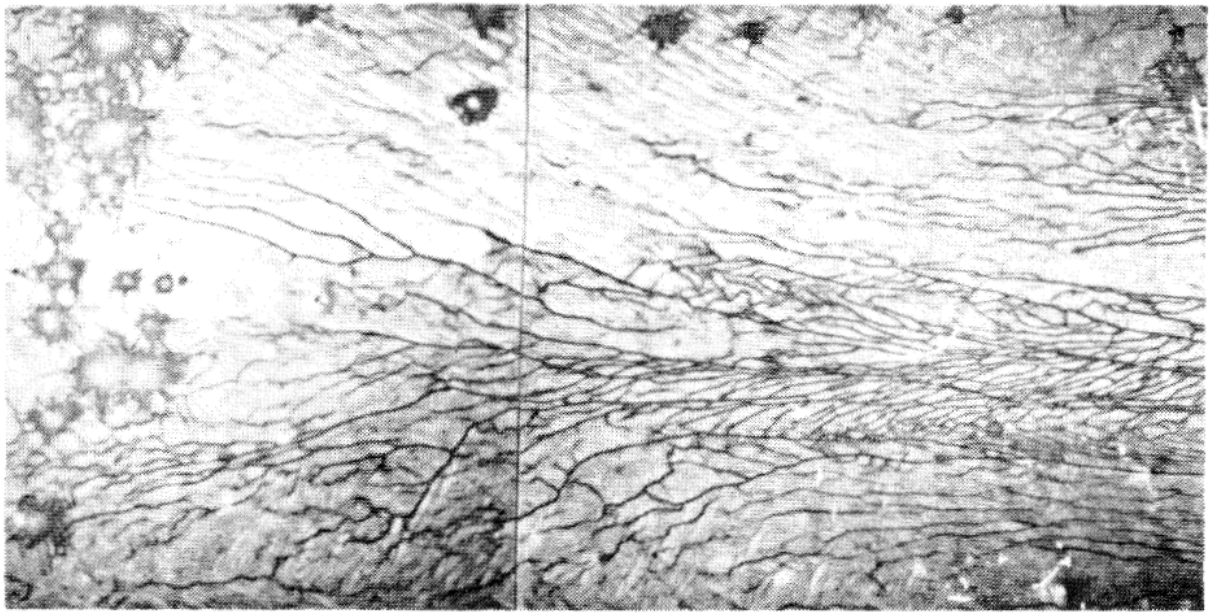

Fig. 2.19. Early stage in the formation of lineage structure in aluminum. Photograph by P. E. Doherty.

→ It is not clear why dislocations of like sign aggregate together when unlike dislocations could annihilate each other, or why similar low-angle boundaries join together instead of annihilating boundaries of opposite tilt.